GLOBAL BIOGEOCHEMICAL CYCLES, VOL. 17, NO. 3, 1084, doi:10.1029/2002GB001968, 2003

Feedbacks between oceanic redox states and marine productivity: A model perspective focused on benthic phosphorus cycling

K. Wallmann
GEOMAR Research Center, Kiel, Germany

Received 8 August 2002; revised 14 March 2003; accepted 20 May 2003; published 16 August 2003

[1] A new model for the marine cycles of particulate organic carbon (POC), oxygen, nitrate, and phosphorus has been developed and applied to explore the controls and constraints on marine productivity and nutrient inventories. The coupled benthic-pelagic model uses a new approach for the simulation of the reactive phosphorus turnover (P_{reac} corresponding to the sum of organic P, authigenic P, and adsorbed phosphate) in marine sediments. The simulated POC/P_{reac} burial ratio in shelf, slope and rise, and deep-sea sediments increases under strongly reducing conditions in agreement with field observation. The model runs revealed that the spread of anoxia in bottom waters may enhance the productivity of the global ocean by one order of magnitude if sufficient nitrate is provided by N_2-fixation. Thus anoxic bottom waters promote eutrophic conditions and vice versa. Additional model runs showed that the productivity and nutrient inventory of the glacial ocean were probably enhanced due to the falling sea level. Marine regression induced a narrowing of the depositional areas on the continental shelves and thereby an increase in the fraction of POC exported to the deep ocean. The accelerated POC delivery, in turn, decreased the oxygen contents of the deep water and thus favored the release of phosphate from deep-sea and rise sediments. Enhanced recycling of phosphate at the seafloor promoted further POC export in a positive feedback loop. *INDEX TERMS:* 1615 Global Change: Biogeochemical processes (4805); 1635 Global Change: Oceans (4203); 3022 Marine Geology and Geophysics: Marine sediments—processes and transport; 3210 Mathematical Geophysics: Modeling; *KEYWORDS:* benthic phosphate fluxes, marine productivity, paleoproductivity, nutrient inventories, redox conditions, feedbacks

Citation: Wallmann, K., Feedbacks between oceanic redox states and marine productivity: A model perspective focused on benthic phosphorus cycling, *Global Biogeochem. Cycles*, *17*(3), 1084, doi:10.1029/2002GB001968, 2003.

1. Introduction

[2] The productivity of the ocean and the marine nutrient inventory are strongly affected by redox-dependent processes [*Lenton and Watson*, 2000; *Redfield*, 1958]. Thus phosphorus is buried in oxic sediments but rapidly released from reducing deposits [*Ingall and Jahnke*, 1994, 1997]. Anoxic conditions favoring the benthic release of phosphate are promoted by high fluxes of particulate organic matter to the seafloor which are in turn controlled by the ocean's productivity. Therefore the phosphorus cycle bears a positive feedback where productivity promotes the release of new phosphate from anoxic sediments inducing a further increase in productivity [*Ingall and Jahnke*, 1994; *van Cappellen and Ingall*, 1994]. In contrast, the ocean's nitrate inventory is affected by denitrification processes occurring both in suboxic sediments and in oxygen-depleted waters [*Gruber and Sarmiento*, 1997]. Under nitrate limitation the ocean's fertility is, thus, stabilized by a negative feedback where enhanced production reduces the nitrate inventory via denitrification processes restoring a moderate level of organic matter production.

[3] Anoxic events where enormous amounts of organic matter accumulated at the seafloor are documented for the mid-Cretaceous, the late Jurassic, and other periods of the Earth's history [*Frakes et al.*, 1992; *Stein et al.*, 1986]. More gradual changes in the ocean's productivity occurred during late Quaternary glacial/interglacial cycles. In many productive areas of the ocean (equatorial Pacific and Atlantic, southern Arabian Sea, sub-Antarctic Ocean), marine surface sediments received more organic carbon and were more reducing under glacial conditions [*Francois et al.*, 1997; *Müller and Suess*, 1979; *Pedersen*, 1983; *Rosenthal et al.*, 1995; *Sarkar et al.*, 1993; *Sarnthein et al.*, 1988; *Thomson et al.*, 1996]. Authigenic U found in glacial sediments throughout the Atlantic implies a basin-wide decrease in the oxygen content of bottom waters during the last glacial [*Mangini et al.*, 2001]. Moreover, benthic and planktonic foraminifer from glacial sediments suggest a larger $\delta^{13}C$ contrast between inorganic carbon dissolved in surface and deep waters implying a more efficient biological pump [*Shackleton et al.*, 1983]. Various mechanisms were advanced to explain the change in productivity suggested by

0886-6236/03/2002GB001968

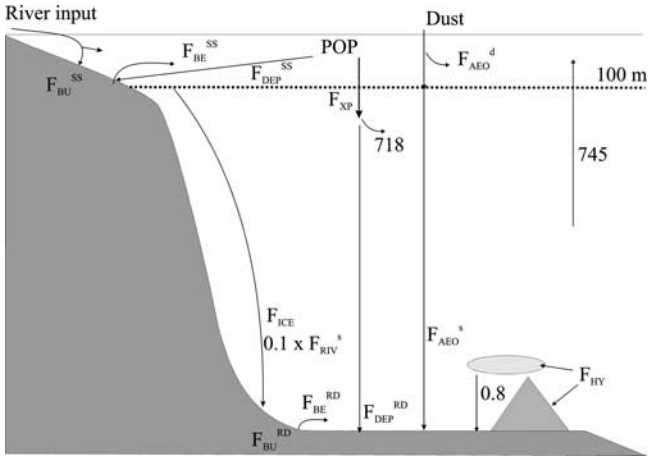

Figure 1. Holocene P turnover in the ocean. Fluxes are defined in Table 1. Numbers indicate additional fluxes in 10^{10} mol P yr^{-1}.

these data [*Archer et al.*, 2000a]. Thus denitrification rates in low-oxygen intermediate waters and underlying slope sediments ceased during glacials [*Altabet et al.*, 1995; *Ganeshram et al.*, 1995] suggesting an increase in the glacial nitrate inventory and in marine productivity [*Falkowski*, 1997; *Falkowski et al.*, 1998]. In contrast, the inventory of dissolved phosphate is generally believed to remain constant over glacial/interglacial cycles even though the geological record suggests that the phosphate inventory may be greatly expanded in low-oxygen waters.

[4] Here a new model for the particulate organic carbon (POC), oxygen, nitrogen, and phosphorus cycling in oceans and sediments is presented. In contrast to previous attempts, the model includes a transport-reaction model for the redox-dependent phosphorus turnover in surface sediments. Sedimentary processes are not only simulated for the deep seafloor but also for the continental margin and shelf considering the terrigenous input of particulate P and POC. The sediment model is fully coupled to a three-box model of the ocean where export production, N_2-fixation, organic matter degradation, and denitrification are the major processes. The coupled model reveals that the positive feedback embedded in the marine phosphorus cycle can induce large changes in the ocean's productivity and nutrient inventory. It also shows that the dissolved phosphate inventory of the ocean may have changed drastically during the Quaternary glacial/interglacial cycles.

2. The Marine Phosphorus Budget

[5] Phosphorus is transferred from the continents into the ocean by rivers, dust, and ice (Figure 1). Preindustrial river fluxes indicate a clear dominance of particulate P over dissolved P inputs [*Meybeck*, 1993]. The particulate load of rivers was strongly enhanced by human land-use even before the onset of industrialization due to large-scale deforestation [*Berner and Berner*, 1996] so that the preanthropogenic flux of particulate P to the ocean was probably close to 33×10^{10} mol yr^{-1} (Table 1). Aeolian inputs provide additional P to the ocean which is partly dissolved in surface waters (1×10^{10} mol P yr^{-1}) and partly deposited at the deep seafloor [2.1×10^{10} mol yr^{-1}; *Duce et al.*, 1991]. Mass transfer rates of terrigenous particles reconstructed by *Lisitzin* [1996] show that similar masses are transported via glacial and aeolian pathways suggesting also a comparable P-flux to the seafloor via glaciers and sea-ice ($\approx 2 \times 10^{10}$ mol yr^{-1}).

[6] Phosphate dissolved in the deep ocean is adsorbed on hydrothermal plume particles suspended in the water column and is bound in altered oceanic crust during hydrothermal circulation of seawater at mid-ocean ridges and ridge flanks [*Wheat et al.*, 1996].

[7] Phosphate dissolved in surface water is readily taken up by plankton to be converted into particulate organic P (POP). The molar ratio between organic carbon and POP in marine algae is given by the classical Redfield ratio [106:1; *Redfield*, 1958]. Estimates of global export production and depositional POC fluxes [*Jahnke*, 1996; *Rabouille et al.*, 2001; *Schlitzer*, 2000; *Yamanaka and Tajika*, 1996] can thus be used to calculate the corresponding POP fluxes [see also *Delaney*, 1998].

[8] Burial of phosphorus in marine sediments can be estimated using total preanthropogenic sediment burial rates [1.55×10^{16} g yr^{-1}; *Lisitzin*, 1996; *Berner and Berner*, 1996] and average P concentrations in marine sediments. Sedimentary P contents typically fall in the range of 0.03–0.13 wt% [*Berner and Rao*, 1994; *Filippelli*, 1997; *Föllmi et al.*, 1993; *Ingall and Jahnke*, 1994; *Ruttenberg*, 1993];

Table 1. Preanthropogenic Fluxes in the Marine Phosphorus Cycle

Flux	Symbol	Value[a]
Particulate riverine P	$F_{RIV}{}^{s}$	33
Dissolved riverine P	$F_{RIV}{}^{d}$	3.2
Particulate aeolian P	$F_{AEO}{}^{s}$	2
Dissolved P release from dust particles	$F_{AEO}{}^{d}$	1
Ice-rafted particulate P	F_{ICE}	2
Removal of dissolved phosphate via hydrothermal processes	F_{HY}	1.4
Marine export production of POP excluding the shelf and slope	F_{XP}	750
Marine POP deposition on the continental shelf and slope	F_{DEP}^{SS}	100
Marine POP deposition on the continental rise and at the deep seafloor	F_{DEP}^{RD}	32
Burial of P in shelf and slope sediments	F_{BU}^{SS}	24
Burial of P in continental rise and deep-sea sediments	F_{BU}^{RD}	12
Benthic release of dissolved P from shelf and slope sediments	F_{BE}^{SS}	106
Benthic release of dissolved P from rise and deep-sea sediments	F_{BE}^{RD}	28

[a]Fluxes are given in 10^{10} mol P yr^{-1}. Preanthropogenic river inputs, aeolian fluxes, ice transport, and hydrothermal fluxes were taken from *Meybeck* [1993], *Berner and Berner* [1996], *Duce et al.* [1991], *Lisitzin* [1996], and *Wheat et al.* [1996], respectively. Marine export production and depositional fluxes were taken from *Schlitzer* [2000], *Yamanaka and Tajika* [1996], *Rabouille et al.* [2001], and *Jahnke* [1996]. Burial rates were calculated from sediment accumulation rates [*Berner and Berner*, 1996; *Lisitzin*, 1996] assuming an average P content of 0.07 wt%. Benthic fluxes of dissolved phosphate were estimated as difference between depositional (POP and inorganic P) and burial fluxes.

with an average estimated here as 0.07 wt%. Considering that two thirds of Holocene sediments (terrigenous and biogenic) accumulate on the continental shelf whereas only one third is deposited on the continental rise and deep seafloor [*Berner and Berner*, 1996; *Lisitzin*, 1996], the corresponding P accumulation rates result as 24×10^{10} and 12×10^{10} mol yr^{-1}, respectively. Phosphorite deposits which contain abundant P (5–40 wt% of P_2O_5) are economically significant but do not act as a relevant P sink in the marine phosphorus cycle [*Berner and Berner*, 1996; *Föllmi et al.*, 1993].

[9] A large fraction of P deposited at the seafloor is released into the pore water due to the microbial degradation of organic matter and the reductive dissolution of manganese and iron oxides [*Colman and Holland*, 2000; *Ingall and Jahnke*, 1997; *McManus et al.*, 1997]. The benthic recycling of dissolved phosphate into the overlying bottom water can be calculated from the difference between depositional flux and burial rate. On the continental shelf and slope, sedimentation is dominated by the deposition of riverine particles and biogenic particles produced in marine surface waters. The resulting P-deposition (130×10^{10} mol P yr^{-1}) is significantly higher than the corresponding P-burial (24×10^{10} mol P yr^{-1}) suggesting a benthic reflux of 106×10^{10} mol P yr^{-1}. P-deposition on the deep seafloor and the continental rise as driven by the sedimentation of POP, riverine, aeolian, glacial, and hydrothermal plume particles (40×10^{10} mol P yr^{-1}) is again significantly higher than the burial flux (12×10^{10} mol P yr^{-1}) resulting in a benthic remobilization of 28×10^{10} mol P yr^{-1}. *Colman and Holland* [2000] used pore water data to calculate benthic phosphate fluxes of 84×10^{10} mol P yr^{-1} for shelf and slope sediments and 41×10^{10} mol P yr^{-1} for sediments deposited at the continental rise and on the deep seafloor. *Hensen et al.* [1998] estimated a global benthic phosphate flux of 32×10^{10} mol P yr^{-1} for water depths >1000 m using a large collection of pore water profiles determined in surface sediments of the southern Atlantic. These independently constrained global fluxes confirm that a large fraction of deposited P is recycled into the overlying water and imply that the benthic fluxes derived here from rain rate and burial data are realistic estimates.

[10] The marine phosphorus budget summarized in Figure 1 and Table 1 has a small and probably insignificant surplus of dissolved P inputs via riverine, aeolian, and benthic processes (138×10^{10} mol P yr^{-1}) over dissolved P removal via POP deposition and hydrothermal processes (133×10^{10} mol P yr^{-1}). Considering the inventory of dissolved P in the global ocean [3.2×10^{15} mol P; *Delaney*, 1998], the residence time of P results as only 2.4 kyr when the benthic release of dissolved phosphate from sediments into the overlying bottom waters is regarded as an input flux to the ocean. Previous budgets of the marine P cycle treat benthic turnover as an internal flux implying significantly larger residence times [*Ruttenberg*, 1993; *Wheat et al.*, 1996]. Benthic fluxes are driven both by the recycling of phosphate previously bound in marine POP and hydrothermal plume particles and by the mobilization of new phosphate from terrigenous particles [*Berner and Rao*, 1994; *Sundby et al.*, 1992] where the later process may release as much as 32×10^{10} mol yr^{-1} of new phosphate into the ocean [*Colman and Holland*, 2000]. Considering this estimate of new phosphate release and the other dissolved phosphate inputs, the residence time of phosphate results as 8.8 kyr. This rather small value clearly indicates that the dissolved phosphate inventory of the ocean may have changed drastically over glacial/interglacial cycles.

3. A New Numerical Model Simulating the Turnover of P, N, POC, and O_2 in the Ocean and in Marine Surface Sediments

[11] Differential equations, flux equations, and parameter values used in the model are summarized in Tables 2–7.

3.1. Pelagic Model

[12] The model setup has been constructed essentially by adding terrigenous and pelagic sediments to the classical three-box model [*Sarmiento and Toggweiler*, 1984; *Siegenthaler and Wenk*, 1984; *Knox and McElroy*, 1984]. In this simple box model, the global ocean is divided into high-latitude and low-latitude surface reservoirs and a deep water box (Figure 2). Thermohaline circulation is imposed as a cyclic flow of 20 Sv [*Toggweiler*, 1999], supplemented by exchange fluxes between individual boxes. In it's standard formulation the three-box model underestimates marine export production considerably [*Archer et al.*, 2000b]. Therefore the vertical and horizontal mixing coefficients were enhanced until the model's export production, oxygen concentrations, and nutrient distributions were close to the conditions observed in the modern ocean (Figure 2). Tuning of mixing coefficients might be justified by the fact that vertical mixing in the real ocean is only poorly constrained [*Archer et al.*, 2000a].

[13] Export production is limited by the least abundant nutrient following Liebig's law (Table 2). It depends on nutrient concentrations as previously defined by *Maier-Reimer* [1993]. Export at high latitudes has a low efficiency expressed by a small value of the kinetic constant k_{XPH} defining the export production at a certain nutrient level. At low latitudes, the corresponding kinetic constant (k_{XPL}) is enhanced to ascertain almost complete consumption of available nutrients. N_2-fixation occurs at low latitudes only. The rate depends on the availability of phosphate [*Sanudo-Wilhelmy et al.*, 2001; *Zehr et al.*, 2001] and is inhibited by high dissolved nitrate concentrations assuming Monod kinetics. It contributes to the export production at low latitudes assuming that 10% of the particulate organic matter (POM) formed by cyanobacteria is exported from the upper layer into the interior of the ocean. Denitrification in the deep water box is driven by export production and is inhibited in the presence of dissolved oxygen; rates are again defined using Monod-type kinetics.

[14] The underlying seafloor is separated into three sections, e.g., continental shelf, margin (slope and rise), and deep seafloor (Figure 2). The seafloor receives POM both from marine export production and from the continents. Terrigenous POC and PON are delivered to the shallow

Table 2. Flux Equations Used in the Model

Parameter	Equation[a]
Export production	$F_{XP} = F_{XPH} + F_{XPL}$
Export production at high latitudes	$F_{XPH} = V_H k_{XPH} \mathrm{Min}\left(\frac{N_H}{16}\frac{N_H}{K_N+N_H}, P_H \frac{P_H}{K_P+P_H}\right)$
Export production at low latitudes	$F_{XPL} = V_L k_{XPL} \mathrm{Min}\left(\frac{N_L}{16}\frac{N_L}{K_N+N_L}, P_L \frac{P_L}{K_P+P_L}\right) + 0.1\frac{F_{NF}}{16}$
N_2-fixation at low latitudes	$F_{NF} = V_L k_{FIX} 16 P_L \frac{P_L}{K_P+P_L}\frac{K_{NF}}{K_{NF}+N_L}$
Denitrification in the deep water column	$F_{DEN} = V_D 106 r_O \frac{4}{5}\frac{K_{O_2}}{O_D+K_{O_2}}\frac{N_D}{N_D+K_{NO_3}}((1-f_{DD}-f_{DR}-f_{DS})F_{XPL} + (1-f_{DD})F_{XPH})$
Depositional P_{reac} fluxes	$0.5\frac{F_{PT,i}}{A_i} + \frac{f_{Di}}{A_i}F_{XP} = \frac{d_S(1-\Phi)}{3.097}\left(-D_{B,i}\frac{\partial PS_i}{\partial x}\Big\vert_{x=0} + w_i PS_i(x=0)\right)$
Depositional POC fluxes	$\frac{F_{POCT,i}}{A_i} + \frac{f_{Di}}{A_i}106F_{XP} = \frac{d_S(1-\Phi)}{1.2}\left(-D_{B,i}\frac{\partial POC_i}{\partial x}\Big\vert_{x=0} + w_i POC_i(x=0)\right)$
Benthic fluxes for dissolved species j	$F_{BE}^{i,j} = A_i \Phi D_{i,j}^S \frac{\partial C_{i,j}}{\partial x}\Big\vert_{x=0}$

[a]Export production (F_{XP}) depends on either nitrate or phosphate concentration considering Liebig's minimum law. It is composed of high-latitude (F_{XPH}) and low-latitude (F_{XPL}) components. Volumes (V_L, V_H) are used to convert concentrations in molar masses and vice versa whereas depositional areas (A_i) are used to define fluxes at the sediment-water interface. The corresponding parameter values are listed in Tables 5 and 6. Depositional fluxes (in mmol cm^{-2} yr^{-1}) are defined as fractions of export production considering additional terrigenous contributions (F_{PT}, F_{POCT}). They are linked to the concentrations (given in wt%) and gradients of sedimentary P and POC providing upper boundary conditions for the benthic model. Benthic fluxes of dissolved species j (oxygen, nitrate, and phosphate) are calculated for each depositional environment i (shelf, slope and rise, deep sea) using the benthic model defined in Table 4. These fluxes are a function of depositional fluxes and affect the concentration of dissolved species in the water column.

seafloor and the continental margin only. In contrast, terrigenous P is distributed between shallow seafloor, continental margin, and deep seafloor considering that about 90% of the riverine inputs are deposited on the continental shelf whereas the eolian and glacial inputs bypass the coastal zone to be exported to the continental slope and rise and deep seafloor (Figure 1).

3.2. Benthic Model

[15] The turnover of dissolved oxygen, nitrate, and phosphate, particulate organic matter (POC), and particulate phosphorus in surface sediments and associated pore waters is simulated with a transport-reaction model using a coupled system of partial differential equations (Table 4). In the model, dissolved species are transported by molecular diffusion. POM and phosphorus are transported by biogenic mixing processes caused by the benthic macrofauna (bioturbation) and via burial, induced by sedimentation. First-order kinetics were applied to simulate both the degradation of POM and the dissolution of reactive P. The kinetic constants were constrained using current estimates of POC burial and POC depositional fluxes [*Betts and Holland*, 1991; *Hedges and Keil*, 1995; *Jahnke*, 1996; *Rabouille et al.*, 2001]. Oxygen consumption and denitrification are driven by POC degradation using Monod kinetics where denitrification is inhibited in the presence of dissolved oxygen [*Boudreau*, 1996; *Rabouille and Gaillard*, 1991; *Van Cappellen and Wang*, 1996].

[16] Phosphorus is separated into reactive and inert fractions where reactive phosphorus (P_{reac}) includes authigenic P-phases, organic P, and other P binding forms subject to

Table 3. Differential Equations Defining the Turnover of Phosphate, Nitrate, and Oxygen in the Water Column

Parameter	Equation[a]
Phosphate in low-latitude surface water	$V_L\frac{dP_L}{dt} = +F_{RIV}^P + F_{AEO}^P - F_{XPL} + 0.5F_{BE}^{PS} + TC(P_D - P_L) + k_{ML}(P_D - P_L) + k_{MHL}(P_H - P_L)$
Phosphate in high-latitude surface water	$V_H\frac{dP_H}{dt} = -F_{XPH} + TC(P_L - P_H) + k_{MH}(P_D - P_H) - k_{MHL}(P_H - P_L)$
Phosphate in deep water	$V_D\frac{dP_D}{dt} = +(1-f_{DD}-f_{DR}-f_{DS})F_{XPL} + (1-f_{DD})F_{XPH} + 0.5F_{BE}^{PS} + F_{BE}^{PR} + F_{BE}^{PD} - k_{HY}V_D P_D + TC(P_H - P_D) - k_{MH}(P_D - P_H) - k_{ML}(P_D - P_L)$
Nitrate in low-latitude surface water	$V_L\frac{dN_L}{dt} = +F_{RIV}^N + F_{AEO}^N + 0.9F_{NF} - 16F_{XPL} + 0.5F_{BE}^{NS} + TC(N_D - N_L) + k_{ML}(N_D - N_L) + k_{MHL}(N_H - N_L)$
Nitrate in high-latitude surface water	$V_H\frac{dN_H}{dt} = -16F_{XPH} + TC(N_L - N_H) + k_{MH}(N_D - N_H) - k_{MHL}(N_H - N_L)$
Nitrate in deep water	$V_D\frac{dN_D}{dt} = +16((1-f_{DD}-f_{DR}-f_{DS})F_{XPL} + (1-f_{DD})F_{XPH}) + 0.5F_{BE}^{NS} + F_{BE}^{NR} + F_{BE}^{ND} - F_{DEN} + TC(N_H - N_D) - k_{MH}(N_D - N_H) - k_{ML}(N_D - N_L)$
Oxygen in deep water	$V_D\frac{dO_D}{dt} = -106r_O\frac{O_D}{O_D+K_{O_2}}((1-f_{DD}-f_{DR}-f_{DS})F_{XPL} + (1-f_{DD})F_{XPH}) + 0.5F_{BE}^{OS} + F_{BE}^{OR} + F_{BE}^{OD} + TC(O_H - O_D) - k_{MH}(O_D - O_H) - k_{ML}(O_D - O_L)$

[a]N_L, N_H, N_D, P_L, P_H, P_D, O_L, O_H, O_D are concentrations of dissolved nitrate (N), phosphate (P), and oxygen (O) in low-latitude surface waters (L), high-latitude surface waters (H), and deep water (D). Additional parameters and parameter values are listed in Table 5. Shelf deposits are mainly located at low- and midlatitudes and extend down to a water depth of 200 m. Therefore they exchange dissolved species both with the low-latitude surface box and the deep water box.

Table 4. Differential Equations Defining the Turnover of POC, P, Oxygen, Nitrate, and Phosphate in Surface Sediments

Parameter	Equation[a]
POC in sediments	$\frac{\partial \mathrm{POC}_i}{\partial t} = D_{B,i}\frac{\partial^2 \mathrm{POC}_i}{\partial x^2} - w_i\frac{\partial \mathrm{POC}_i}{\partial x} - k\mathrm{POC}_i$
Reactive P in sediments	$\frac{\partial \mathrm{PS}_i}{\partial t} = D_{B,i}\frac{\partial^2 \mathrm{PS}_i}{\partial x^2} - w_i\frac{\partial \mathrm{PS}_i}{\partial x} - k\alpha\left(1-\frac{\mathrm{PO}_4^i}{\mathrm{PO}_4^{\mathrm{SAT}}}\right)\mathrm{PS}_i + k_{\mathrm{up}}\mathrm{PO}_4^i\frac{\Phi 3.097}{d_S(1-\Phi)}\frac{\mathrm{NO}_3^i}{\mathrm{NO}_3^i+K_{\mathrm{NO}_3}}$
Oxygen in pore water	$\frac{\partial \mathrm{O}_2^i}{\partial t} = D_{\mathrm{O}_2,i}\frac{\partial^2 \mathrm{O}_2^i}{\partial x^2} - k\mathrm{POC}_i r_O\frac{d_S(1-\Phi)}{1.2\Phi}\frac{\mathrm{O}_2^i}{\mathrm{O}_2^i+K_{\mathrm{O}_2}}$
Nitrate in pore water	$\frac{\partial \mathrm{NO}_3^i}{\partial t} = D_{\mathrm{NO}_3,i}\frac{\partial^2 \mathrm{NO}_3^i}{\partial x^2} + k\mathrm{POC}_i r_N\frac{d_S(1-\Phi)}{1.2\Phi}\frac{\mathrm{O}_2^i}{\mathrm{O}_2^i+K_{\mathrm{O}_2}} - k\mathrm{POC}_i r_{\mathrm{DN}}\frac{d_S(1-\Phi)}{1.2\Phi}\frac{K_{\mathrm{O}_2}}{\mathrm{O}_2^i+K_{\mathrm{O}_2}}\frac{\mathrm{NO}_3^i}{\mathrm{NO}_3^i+K_{\mathrm{NO}_3}}$
Phosphate in pore water	$\frac{\partial \mathrm{PO}_4^i}{\partial t} = D_{\mathrm{PO}_4,i}\frac{\partial^2 \mathrm{PO}_4^i}{\partial x^2} + k\alpha\left(1-\frac{\mathrm{PO}_4^i}{\mathrm{PO}_4^{\mathrm{SAT}}}\right)\mathrm{PS}_i\frac{d_S(1-\Phi)}{3.097\Phi} - k_{\mathrm{up}}\mathrm{PO}_4^i\frac{\mathrm{NO}_3^i}{\mathrm{NO}_3^i+K_{\mathrm{NO}_3}}$

[a]Dissolved oxygen, nitrate, and phosphate concentrations in pore waters are given in mmol $(\mathrm{cm}^3 \text{ pore water})^{-1}$, reactive P and POC concentrations are calculated in wt%. The five differential equations describing the benthic processes are solved for three different depositional areas. The index i in these equations stands for D (deep sea), R (continental rise and slope), and S (shelf). The corresponding parameter values are listed in Table 6. The upper boundary conditions of the benthic P and POC models are given by the corresponding depositional fluxes (Table 2) provided by the pelagic model (Table 3) whereas the upper boundary of the pore water models for oxygen, nitrate, and phosphate are given by the corresponding concentrations in the overlying water reservoirs also calculated in the pelagic box model (Table 3). These fluxes and concentrations change through time providing a dynamic upper boundary for the benthic model and a close benthic-pelagic coupling. Shelf bottom water concentrations were calculated as averages of deep water and low-latitude surface water concentrations. Zero gradients are used as lower boundary condition at the bottom of the modeled sediment column (10 cm sediment depth).

rapid diagenesis in surface sediments. Nonreactive, inert P (P_{in}, mainly apatite) is delivered from the continents assuming that 50% of the total terrigenous input is inert. The model considers only reactive P. Degradation kinetics of P_{reac} are based on the observation that reactive P is more labile than POC [*Ingall and Van Cappellen*, 1990] and that secondary P-bearing minerals are formed via precipitation of phosphate from pore waters:

$$R_D = -k\alpha\left(1-\frac{\mathrm{PO}}{\mathrm{PO}_4^{\mathrm{SAT}}}\right)\mathrm{PS}.$$

[17] Here the degradation/dissolution rate (R_D) depends on P_{reac} concentrations (PS) and on dissolved phosphate concentrations (PO_4) in associated pore waters. The same first-order kinetic constant (k) is used for both the degradation of POC and P_{reac}. The constant α which may attain values in between 1 and 3 expresses the preferential degradation of organic P as well as phosphate mobilization due to the reductive dissolution of metal oxides and desorption processes [*Berner and Rao*, 1994; *Sundby et al.*, 1992]. A saturation concentration (PO_4^{SAT}) is introduced to consider the decrease in net dissolution at high dissolved phosphate levels due to the formation of authigenic minerals. Calcium carbonate fluorapatites (CFA) act as major control on dissolved phosphate allowing for high steady state concentrations due to sluggish precipitation kinetics and/or the formation of amorphous phases [*Reimers et al.*, 1996; *Ruttenberg and Berner*, 1993]. In the model, the saturation concentration of phosphate is set to 500 μM so that dissolution of particulate P is inhibited when the calculated concentrations approach the saturation value.

[18] The incorporation of P by aerobic bacteria and the uptake of dissolved phosphate via adsorption on metal

Table 5. Parameter Values of the Pelagic Model Used for the Holocene Simulation[a]

Parameter/Symbol	Value	Reference
Volume of low-latitude box V_L, m^3	2.97×10^{16}	[*Toggweiler*, 1999]
Volume of high-latitude box V_H, m^3	1.31×10^{16}	[*Toggweiler*, 1999]
Volume of deep water box V_D, m^3	1.249×10^{18} (1.208×10^{18})	[*Toggweiler*, 1999]
Kinetic constant for export production at low latitudes k_{XPL}, yr^{-1}	10	this work
Kinetic constant for export production at high latitudes k_{XPH}, yr^{-1}	0.15 (0.20–0.30)	this work
Monod constants for export production K_N, K_P, μM	0.01	this work
Kinetic constant for N_2-fixation at low latitudes k_{FIX}, yr^{-1}	10	this work
Monod constant for N_2-fixation at low latitudes K_{NF}, μM	0.1	this work
Riverine input of dissolved P $F_{\mathrm{RIV}}^{\mathrm{P}}$, mol yr^{-1}	3.2×10^{10}	[*Meybeck*, 1993]
Release of dissolved P from aeolian dust $F_{\mathrm{AEO}}^{\mathrm{P}}$, mol yr^{-1}	1×10^{10} (2×10^{10})	[*Duce et al.*, 1991]
Kinetic constant for hydrothermal phosphate uptake k_{HY}, yr^{-1}	6×10^{-6}	[*Wheat et al.*, 1996]
Riverine input of dissolved N $F_{\mathrm{RIV}}^{\mathrm{N}}$, mol yr^{-1}	1×10^{12}	[*Meybeck*, 1993]
Eolian input of dissolved N $F_{\mathrm{AEO}}^{\mathrm{N}}$, mol yr^{-1}	2×10^{12}	[*Cornell et al.*, 1995]
Molar ratio between oxygen consumption and POC degradation rate r_O	1.4	[*Anderson and Sarmiento*, 1994]
Oxygen concentration in low-latitude surface water O_L, μM	250	this work
Oxygen concentration in high-latitude surface water O_H, μM	350	this work

[a]Glacial values are given in parenthesis.

Table 6. Parameter Values Used in the Modeling of Sedimentary Processes in Different Depositional Environments[a]

Parameter	Deep Sea	Slope and Rise	Shelf	References
Area of the seafloor A, m^2	280×10^{12}	53×10^{12}	29×10^{12}(15×10^{12})	[*Menard and Smith*, 1966]
Sediment accumulation rate, g yr^{-1}	2.0×10^{15} (3.5×10^{15})	3.2×10^{15}(13×10^{15})	10.3×10^{15} (2×10^{15})	[*Berner and Berner*, 1996; *Lisitzin*, 1996]
Sedimentation rate w, cm kyr^{-1}	1.4 (2.4)	11 (45)	68 (26)	this work
Fraction of export production deposited at the seafloor f_{Di}[b]	0.021	0.03	0.14 (0.07)	[*Jahnke*, 1996; *Rabouille et al.*, 2001]
Depositional flux of terrigenous P F_{PT}, mol yr^{-1}	1×10^{10} (4×10^{10})	6×10^{10} (34×10^{10})	30×10^{10} (3×10^{10})	this work
Depositional flux of terrigenous POC F_{POCT}, mol yr^{-1}	0	1×10^{12} (7×10^{12})	7×10^{12} (1×10^{12})	this work
Bioturbation coefficient D_B, cm^2 yr^{-1}	1	5	25	[*Middelburg et al.*, 1996a]
Diffusion coefficient of oxygen in sediments D_{O_2} cm^2 yr^{-1}	274	274	548	[*Boudreau*, 1997]
Diffusion coefficient of nitrate in sediments D_{NO_3} cm^2 yr^{-1}	224	224	448	[*Boudreau*, 1997]
Diffusion coefficient of phosphate in sediments D_{PO_4} cm^2 yr^{-1}	97	97	194	[*Boudreau*, 1997]
Kinetic constant for POC and P_{reac} degradation k, yr^{-1}	0.02	0.02	0.06	this work
Kinetic constant for phosphate uptake k_{up}, yr^{-1}	55	55	165	this work
Saturation concentration of PO_4 in pore water PO_4^{SAT}, μM	500	500	500	this work
Preferential degradation of P_{reac} versus POC α	2	2	2	this work
Monod constants K_{O_2}, K_{NO_3}, μM	1	1	1	this work
Porosity Φ	0.8	0.8	0.8	this work
Density of dry solids d_S, g cm^{-3}	2.6	2.6	2.6	this work

[a]Glacial values are given in parenthesis.
[b]Deep sea, fraction of F_{XP}; slope and rise and shelf, fraction of F_{XPL}.

oxides and coprecipitation with newly formed Mn(IV)- and Fe(III)-oxides and hydroxides are considered using the following kinetic equation:

$$R_{UP} = k_{up}PO_4\, f_S \frac{NO_3}{NO_3 + K_{NO_3}},$$

where the phosphate uptake rate (R_{UP}) depends on the prevailing concentration of dissolved phosphate and the presence of dissolved nitrate (NO_3) using first-order kinetics and Monod kinetics, respectively. The stoichiometric factor f_S is introduced to convert dissolved phosphate concentrations into solid phase concentrations of reactive P considering sediment density and water contents. With this formulation phosphate uptake is limited to nitrate-bearing surface sediments as suggested by various field studies [*Colman and Holland*, 2000; *Ingall et al.*, 1993; *Ingall and Jahnke*, 1994; *Sundby et al.*, 1992]. Thus benthic P fluxes are mainly controlled by the redox conditions in surface sediments [*Colman and Holland*, 2000] which are in turn regulated by the deposition of organic matter to the seafloor and by the oxygen content of the overlying bottom waters [*Ingall and Jahnke*, 1997].

[19] The benthic model is applied to simulate the turnover in the top 10 cm of deep sea, continental rise and slope, and continental shelf sediments using parameter values listed in Table 6. The bioturbation coefficients are calculated using an empirical relation to water depths based on ^{210}Pb data [*Middelburg et al.*, 1996a]. Sedimentation rates are estimated for the different environments considering the corresponding mass fluxes, depositional areas, an average porosity of 80%, and a density of dry solids of 2.6 g/cm^3 [*Berner and Berner*, 1996; *Colman and Holland*, 2000; *Lisitzin*, 1996]. Molecular diffusion coefficients of dissolved species in

Table 7. Model Equations Used in section 4.4

Parameter	Equation
Burial of particulate organic N	$F_{BN} = \frac{d_S(1-\Phi)16}{1.2\times106}(A_D w_D POC_D(L) + A_R w_R POC_R(L) + 0.5A_S w_S POC_S(L))$
Ammonia in deep water	$V_D \frac{dNH_D}{dt} = +\frac{K_{O_2}}{O_D+K_{O_2}} \frac{K_{NO_3}}{N_D+K_{NO_3}}(16(F_{XPL}(1-0.5f_{DS}) + F_{XPH}) - F_{BN}) - NH_D(TC + k_{MH} + k_{ML})$
Nitrate in low-latitude surface water	$V_L \frac{dN_L}{dt} = +F^N_{RIV} + F^N_{AEO} + 0.9F_{NF} - 16F_{XPL} + 0.5F^{NS}_{BE} + TC(N_D + NH_D - N_L) + k_{ML}(N_D + NH_D - N_L) + + k_{MHL}(N_H - N_L)$
Nitrate in high-latitude surface water	$V_H \frac{dN_H}{dt} = -16F_{XPH} + TC(N_L - N_H) + k_{MH}(N_D + NH_D - N_H) - k_{MHL}(N_H - N_L)$
Bioturbation coefficients in deep-sea, rise and shelf sediments	$D_{B,D} = 1\frac{O_D}{K_{O_2}+O_D} \quad D_{B,R} = 5\frac{O_D}{K_{O_2}+O_D} \quad D_{B,S} = 25\frac{(O_L+O_D)/2}{K_{O_2}+(O_L+O_D)/2}$

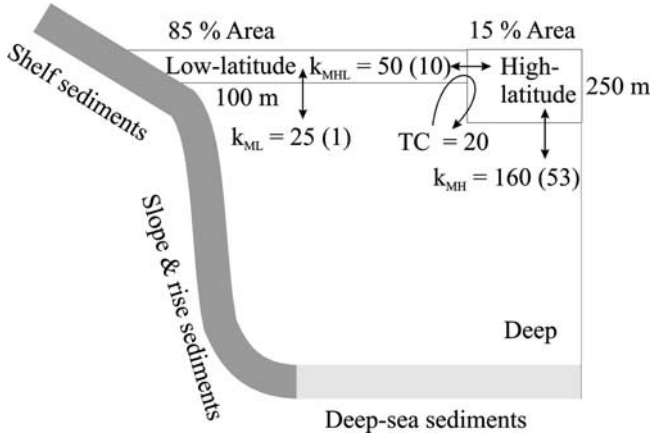

Figure 2. Model setup. The ocean is represented by the conventional three-box model of the ocean [*Sarmiento and Toggweiler*, 1984; *Siegenthaler and Wenk*, 1984; *Knox and McElroy*, 1984]. Global circulation is represented by a cyclic flow (TC = 20 Sv) as well as by vertical and horizontal mixing coefficients (in Sv = 10^6 m^3 s^{-1}). Mixing is enhanced to allow for realistic export production and deep-water ventilation. Original data [*Archer et al.*, 2000b; *Toggweiler*, 1999] are given in brackets. The seafloor is divided into deep sea, margin (rise and slope), and shelf. Terrigenous sediments, organic matter, and nutrients are added to the oceans via rivers, glaciers, and dust deposition.

deep-sea and margin sediments are calculated for the given porosity and the prevailing low temperatures (2°–4°C) using empirical equations [*Boudreau*, 1997]. For continental shelf sediments, the values of the diffusion coefficients are increased to account for higher bottom water temperatures and the enhanced transport of dissolved species via bioirrigation.

[20] The sediment model is closely coupled to the water column boxes. It receives marine POM from surface waters, it consumes dissolved oxygen and nitrate from bottom waters and releases dissolved phosphate and nitrate into the overlying water column. Continental shelf and margin deposits receive POM produced in the low-latitude surface box only because continents are mainly located at low- and midlatitudes. In contrast, the deep seafloor is supplied with organic matter from both high and low latitudes. The continental shelf extends down to a water depth of 200 m. Therefore the benthic exchange between shelf sediments and overlying bottom water affects both low-latitude surface water and deep-water concentrations.

[21] The system of 7 ordinary and 15 partial differential equations defined in Tables 3 and 4 was solved using finite difference techniques as implemented in the commercial software MATHEMATICA. The object NDSolve which was applied to integrate the differential equations uses the numerical procedure "Method of Lines." This procedure based on partial discretization has been successfully applied in previous modeling of benthic processes [*Boudreau*, 1996, 1997; *Luff et al.*, 2000]. A high depth resolution (0.05 cm at the surface of shelf sediments) was used in the sediment model to minimize numerical errors and determine reliable benthic fluxes. Mass balances for sediment and water species indicate that the numerical errors were small so that masses were conserved almost completely (mass balance errors <0.01%). A typical steady state run was completed within 1 hour on a PC with Pentium IV processor whereas nonsteady state calculations were numerically more demanding. MATHEMATICA notebooks containing the full model code are available on request.

4. Results and Discussions

[22] The results of different model applications are presented and discussed in the following section. In the first paragraph, the coupled benthic-pelagic model is calibrated by fitting the model to the fluxes and nutrient concentrations observed in the modern ocean. Subsequently, the sensitivity of the benthic model is tested and the results are compared to field data. In the third paragraph the coupled benthic-pelagic model is used to constrain the productivity of the glacial ocean and in the final paragraph the model is applied to explore the upper limits of marine productivity.

4.1. Simulating the Turnover of POC, Nutrients, and Dissolved Oxygen in the Prehuman Holocene Ocean

[23] The model was run repeatedly using different parameter values for the preferential degradation of reactive P (α = 1–3), phosphate uptake in nitrate-bearing surface sediments (k_{up} = 20–200 yr^{-1}), and N_2-fixation (k_{FIX} = 0.1–10 yr^{-1}, K_{NF} = 0.01–1 μM) until the resulting steady state fluxes and concentrations were consistent with available observations. The most realistic results were obtained using the parameter set listed in Tables 5 and 6 (k_{up} = 55 yr^{-1} for deep-sea and margin sediments, k_{up} = 165 yr^{-1} for shelf sediments, α = 2 for all sediments, k_{FIX} = 10 yr^{-1}, K_{NF} = 0.1 μM). The resulting concentrations in surface and deep waters, as well as export productions, depositional fluxes, and rates of benthic turnover (Tables 8 and 9) are close to observations (Figure 1 and Table 1) demonstrating that the model presented here can be used to simulate the marine POC, N, P, and O_2 cycles.

[24] Turnover of nitrogen occurred mainly via denitrification in shelf sediments and N_2-fixation in low-latitude surface waters. Denitrification was forced by high rates of POC deposition at shallow water depths which lead to rapid oxygen depletion in sediment pore waters and high rates of sedimentary denitrification falling into the range of recent estimates [*Middelburg et al.*, 1996b]. N_2-fixation was controlled by the availability of dissolved phosphate in low-latitude surface waters and was inhibited by high levels of dissolved nitrate. The atomic N/P ratio in surface waters at low latitudes was effectively stabilized to a value corresponding to observations (15) using the appropriate combination of parameter values (k_{FIX} = 10 yr^{-1}, K_{NF} = 0.1 μM). The resulting N_2-fixation rate is two times higher than a recent estimate derived from field observations [*Gruber and Sarmiento*, 1997]. The field data are controversial but suggest that the nitrogen cycle might have been out of steady state during late Quaternary glacial/interglacial cycles [*Codispoti*, 1995]. This scenario is not explored in the simulations because the model was run into

Table 8. Pelagic Model Results for the Preanthropogenic Holocene

Parameter	Low-Latitude Surface Water	High-Latitude Surface Water	Deep Water
Oxygen concentration, μM	250[a]	350[a]	183
Nitrate concentration, μM	0.39	17	31
Phosphate concentration, μM	0.025	1.3	2.2
N/P ratio (atomic)	15	13	14
Export production, Tmol POC yr^{-1}[b]	584	219	
N_2-fixation, Tmol N yr^{-1}	18		
Denitrification, Tmol N yr^{-1}			4

[a]Prescribed value.
[b]1 Tmol = 10^{12} mol.

steady state to calibrate unknown parameter values with available observations.

[25] The ratio between organic carbon mineralization in surface sediments and benthic phosphate fluxes into the overlying bottom water increased with water depth (last row in Table 9). The ratio was higher than the Redfield ratio (106) in average deep-sea sediments due to the large nitrate penetration depth and the enhanced removal of dissolved phosphate within surface sediments. This model result is again consistent with field observations [*Colman and Holland*, 2000; *Hensen et al.*, 1998; *Smith et al.*, 1979].

[26] P_{reac} burial efficiency, i.e., the ratio between total P_{reac} burial (organic and terrigenous P) and depositional rate varied only moderately between deep sea, continental margin, and shelf whereas POC burial efficiency was strongly enhanced with decreasing water depth, increasing sedimentation rate, and POC deposition as previously observed [*Betts and Holland*, 1991; *Müller and Suess*, 1979; *Sarnthein et al.*, 1988].

[27] Resulting sediment and pore water profiles show the typical features observed in marine surface sediments (Figure 3): POC concentrations strongly decrease with water depths whereas oxygen penetration depths are enhanced due to the lower POC depositional flux in deep water areas. The P_{reac} content is only weakly affected by water depths and depositional fluxes because the enhanced mobilization of dissolved P compensates for the elevated rain rate of particulate P to sediments at shallow water depths. The pore water concentrations of dissolved phosphate are low in the presence of dissolved oxygen and nitrate. They increase strongly below the nitrate penetration depth due to diminished removal under anoxic conditions as observed in many field studies [*Christensen*, 1987; *Sundby et al.*, 1992].

4.2. Controls on Burial Rates and Benthic Phosphate Fluxes

[28] The sensitivity of the benthic model to changes in sedimentary redox conditions was explored in a large number of model runs. The depositional fluxes of POC and the oxygen concentrations prevailing in the overlying bottom waters were varied systematically and the benthic model was run into steady state to calculate the resulting burial rates and benthic fluxes of organic carbon, reactive phosphorus, and dissolved phosphate. In these model runs, bioturbation coefficients were diminished when the oxygen concentrations in the overlying bottom water decreased below a critical value of 20 μM. Moreover, the depositional flux of reactive P (F_{dep}^{Pr}) was varied according to:

$$F_{dep}^{Pr}\left(F_{dep}^{POC}\right) = 0.5F_{dep}^{PT} + \frac{F_{dep}^{POC}}{106},$$

where F_{dep}^{PT} is the depositional rate of terrigenous P normalized to the corresponding seafloor area whereas F_{dep}^{POC} is the rate of POC deposition systematically varied in

Table 9. Benthic Model Results for the Preanthropogenic Holocene

Parameter	Shelf Sediments	Slope and Rise Sediments	Deep-Sea Sediments
Depositional POC flux, Tmol yr^{-1}	89	19	17
Depositional PON flux, Tmol yr^{-1}	12	2.6	2.5
Depositional P_{reac} flux, 10^{10} mol yr^{-1}	92	20	16
Benthic nitrate flux, Tmol NO_3 yr^{-1}	0.6	−0.1[a]	2.2
Benthic phosphate flux, 10^{10} mol yr^{-1}	75	16	15
Denitrification rate, Tmol N yr^{-1}[b]	10	2.6	0.4
POC burial, Tmol yr^{-1}	8.7	0.9	0.08
POC burial efficiency, %	10	5	0.5
P_{reac} burial, 10^{10} mol yr^{-1}	17	3	1
P_{reac} burial efficiency, %	19	17	8
Deposition and burial of P_{in}, 10^{10} mol yr^{-1}	15	3	0.5
Benthic C:P flux ratio, atomic[c]	107	109	111

[a]The negative sign denotes a flux from the bottom water into the sediment.
[b]Calculated from mass balances considering depositional inputs, benthic NO_3 fluxes, and N burial rates.
[c]Ratio between depth-integrated POC degradation in the upper 10 cm of the sediment column and benthic phosphate flux.

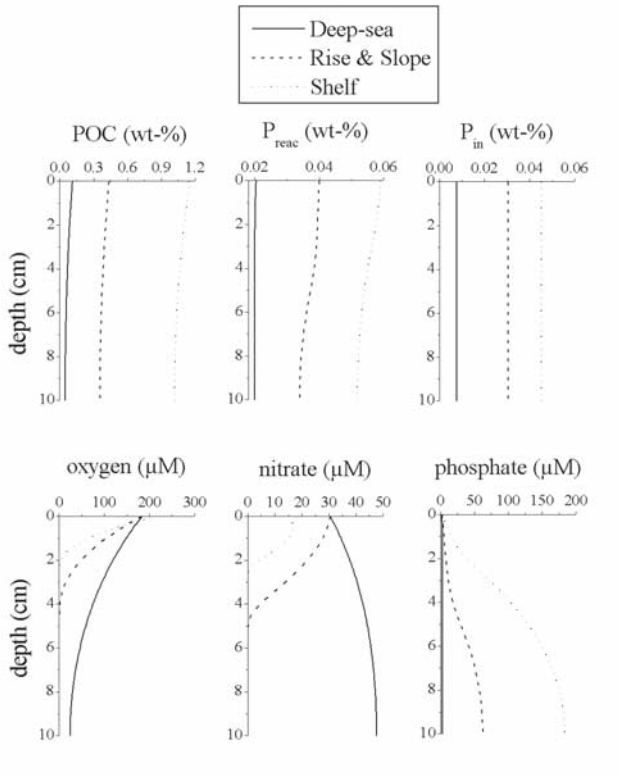

Figure 3. Benthic model results for the preanthropogenic Holocene at steady state. Depth profiles of particulate organic carbon (POC), reactive phosphorus (P_{reac}), inert phosphorus (P_{in}), dissolved oxygen, nitrate, and phosphate in sediment pore waters are shown for the three different depositional environments considered in the model (deep-sea, slope and rise, shelf).

the simulations. Finally, additional simulations were run using zero concentrations of both oxygen and nitrate in the bottom water to mimic completely anoxic conditions. Approximately, 50 model runs were performed for each of the three depositional environments. The model results for the slope and rise environment are presented in Figure 4.

[29] The ratio between burial of POC and P_{reac} changed strongly as a function of both bottom water oxygen concentrations and depositional POC fluxes (Figure 4). Low ratios corresponding to the recent values occurred under oxic conditions with well-ventilated bottom waters and low to moderate POC fluxes. Under these conditions the uptake of dissolved phosphate in nitrate-bearing surface sediments significantly enhanced the P_{reac} contents of solids and thus the P_{reac} burial rates. Low ratios were also obtained with oxygen-depleted bottom waters under extremely eutrophic conditions. In this situation, the P_{reac} burial was enhanced because the dissolved phosphate concentrations in the pore fluids approached the saturation level (500 µM) inhibiting any further release of phosphate from the sediment. Very high ratios occurred under anoxic bottom waters and eutrophic conditions. In this setting, the phosphate uptake in surface sediments was inhibited because the overlying bottom waters contained neither oxygen nor dissolved nitrate. Moreover, dissolved phosphate concentrations at depth did not approach the saturation level due to the moderate rates of POC and P_{reac} deposition. The preferential degradation of P_{reac} with respect to POC, as defined by the model parameter α, then dominated the benthic turnover inducing extremely high-POC/P_{reac} burial ratios.

[30] The sensitivity of the model with respect to productivity and redox mimics the trends observed in marine sediments. Thus the POC/P_{reac} ratios in deep-sea and rise sediments generally increase with POC contents and productivity [*Anderson et al.*, 2001] and sediments with high-POC/P_{reac} ratios are common in marginal seas with periodic or permanently anoxic bottom waters [*Arthur and Dean*, 1998; *Emeis et al.*, 2000]. Moreover, fossil-laminated shales deposited under anoxic conditions have atomic POC/POP ratios of up to 3900 [*Ingall et al.*, 1993]. In contrast, extremely productive continental margins such as the Peruvian shelf and slope often produce P_{reac}-rich deposits (phosphorites) with low-POC/P_{reac} ratios. The genesis of

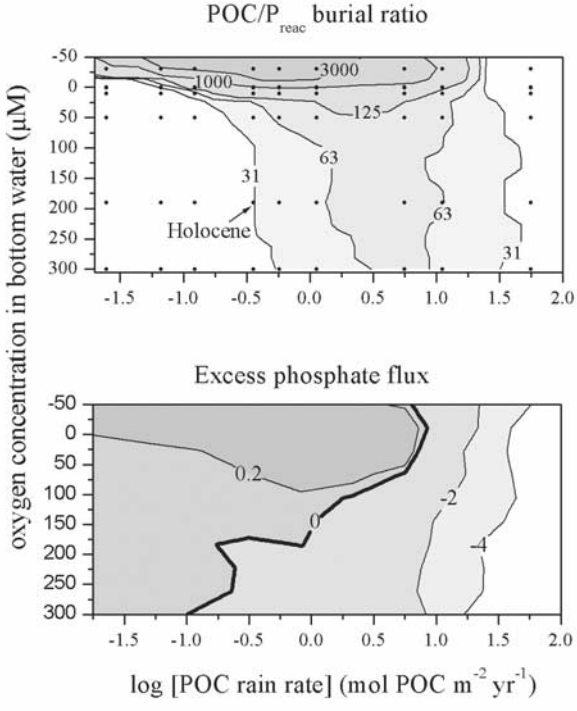

Figure 4. Sensitivity of the phosphorus turnover in continental slope and rise sediments toward changes in POC depositional fluxes and oxygen contents of bottom waters. (top) Atomic ratio of POC burial and reactive P burial. (bottom) excess benthic phosphate fluxes at the sediment-water interface (in mmol P m^{-2} yr^{-1}). POC/P_{reac} burial ratios and benthic fluxes were calculated in 54 consecutive model runs shown as dots in top panel. Contour lines were produced using procedures implemented in ORIGIN 6.1. Negative oxygen concentrations represent anoxic bottom waters depleted in dissolved nitrate. Parameter values were set as defined in Table 6.

these economically important deposits is also affected by bottom currents and other factors that are not considered in the model [*Van Cappellen and Berner*, 1988]. Nevertheless, the low-POC/P_{reac} ratios produced by the model under extremely eutrophic conditions reflect the major effect observed in this setting.

[31] The redox-dependent recycling of phosphate in surface sediments is also reflected in the benthic fluxes of dissolved phosphate at the sediment-water interface. An excess flux of phosphate (F_{ben}^{ex}) was calculated from the total benthic phosphate flux (F_{ben}^{tot}) and the depth-integrated rate of organic matter degradation (R_{POC}) as:

$$F_{ben}^{ex} = F_{ben}^{tot} - \frac{R_{POC}}{106}.$$

[32] This excess flux represents the non-Redfieldian component of the total phosphate flux. Positive excess fluxes are due to the mobilization of new dissolved phosphate from reactive terrigenous phosphorus phases and are also induced by the preferential degradation of phosphorus-bearing organic substances whereas negative excess fluxes are caused by the uptake of phosphate by benthic microorganisms, via adsorption and mineral formation.

[33] As expected, the excess fluxes mirror the pattern revealed already in the POC/P_{reac} burial ratios. Thus large positive fluxes occur under reducing conditions and at moderate productivity. Again, in situ flux data as well as pore water data from dominantly anoxic deposits confirm that these sediments generally release excess phosphate into the overlying bottom water [*McManus et al.*, 1997; *Colman and Holland*, 2000; *Balzer*, 1984]. In situ flux data from marginal basins and continental slope sites [*Berelson et al.*, 1987; *Ingall and Jahnke*, 1997; *McManus et al.*, 1997; *Reimers et al.*, 1992] revealed negative excess fluxes at oxygen concentrations above 50 μM and positive fluxes at oxygen values below 20 μM.

4.3. Constraining the Productivity of the Glacial Ocean

[34] The low-glacial sea level exerts a strong influence on the patterns of terrigenous sedimentation and affects sedimentary processes on the continental shelf which could in turn change the nutrient contents of seawater. Thus *McElroy* [1983] proposed that diminished denitrification on continental shelves enhanced the glacial nitrate inventory whereas *Broecker* [1982] suggested that the glacial phosphate inventory was enlarged due to diminished sedimentation and burial of particulate phosphorus in shelf deposits. During the Holocene, the fraction of riverine particles deposited on the continental shelf is high (90%) because the shelf is not at isostatic equilibrium with the present sea level but is still affected by the much lower glacial sea level [*Hay and Southam*, 1977]. Under glacial conditions, the anomalous Holocene rate was diminished by an order of magnitude [*Hay*, 1994] shifting the focus of sedimentation from the shelf to the continental rise and slope. The glacial sea level was ~120 m below its present value [*Rohling et al.*, 1998] reducing the water-covered shelf and marginal sea areas by approximately 50% [*Ludwig et al.*, 1999; *Menard and Smith*, 1966; *Peltier*, 1994]. Moreover, the transport of ice-rafted material to the margin and the deposition of aeolian dust at the deep seafloor were strongly enhanced increasing the total sedimentation rate by approximately 3×10^{15} g yr^{-1} [*Lisitzin*, 1996]. The increased dust input also enhanced the release of dissolved phosphate from dust particles and thereby the input of dissolved phosphate into the ocean. Changes in sedimentation rate, water volume, depositional areas, terrigenous inputs, and dust delivery which likely occurred under glacial conditions are summarized in Tables 5 and 6.

[35] The model was run with these new parameter values to simulate the nutrient turnover under glacial conditions (simulation G1 in Figure 5). The new steady state is characterized by slightly higher inventories of nitrate and phosphate, an enhanced export productivity, and diminished oxygen concentrations in deep water with respect to the Holocene simulation. Subsequently, the fraction of total export production deposited on the continental shelf was diminished (simulations G2–G6). This change is suggested by the strong decrease in the depositional areas at shallow water depths induced by the marine regression. It is reasonable to assume that a smaller fraction of total export production was deposited on narrower glacial shelves so that a correspondingly larger fraction of export production was degraded in the water column. The enhanced water column respiration induced lower oxygen contents in the deep water box (Figure 5b) which in turn induced a more efficient recycling of dissolved phosphate in deep-sea and margin sediments and thereby an increase in the phosphate inventory (Figure 5c). Higher phosphate concentrations favored N_2-fixation at low latitudes inducing an increase in the dissolved nitrogen inventory (Figure 5c) which finally enhanced the marine productivity (Figure 5a). The atomic N/P ratio in average seawater was maintained close to it's current value (15) because the model compensated for enhanced phosphate levels by enhanced N_2-fixation rates. Below a certain threshold value in the oxygen concentration of deep water (≈100 μM), a gradual change in POC deposition induced an enormous jump in productivity and thereby an almost complete consumption of oxygen in the deep water box (simulation G4). This nonlinear behavior is due to the feedbacks embedded in the model formulation. An increase in productivity removes phosphate and nitrate from surface waters into the deep ocean and the underlying sediments. This negative feedback keeps the productivity at a moderate level during simulations H, G1, G2, and G3. At a certain threshold, the negative feedback is overcome by a positive feedback founded in the redox-dependence of benthic phosphate recycling. Under these conditions, an increase in productivity promotes sufficiently anoxic conditions in surface sediments which strongly enhance the benthic reflux of phosphate into the ocean and thereby the marine productivity. The positive feedback accelerates export production until N_2-fixation no longer compensates for the concurrent increase in denitrification. Nitrate is then not only the proximate but also the ultimate limiting nutrient. The nitrate inventory in the deep ocean declines rapidly due to the ongoing denitrification (Figure 5c) but the export production is maintained at a high level due to the ongoing

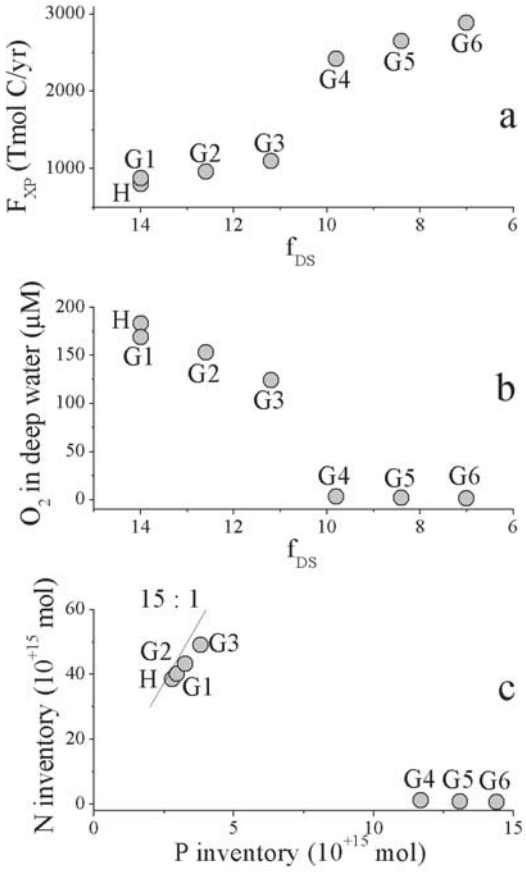

Figure 5. Productivity, redox state, and nutrient inventory of the glacial ocean as affected by the decreasing POC deposition on continental shelves. (a) Total export production (from high- and low-latitude surface waters) as a function of the fraction of export production at low-latitudes deposited on the continental shelves (f_{DS}). (b) Oxygen concentrations in the deep water box as function of f_{DS}. (c) Total nitrate and phosphate contents of the ocean (surface and deep water boxes) at different f_{DS} values. Each point represents the result of an individual model run produced with a certain set of parameter values. Simulations were continued until export production, nutrient inventories, and oxygen concentrations reached a steady state. *H* stands for the Holocene simulation, a complete list of the model parameters is given in Tables 5 and 6. G1 is the first simulation for glacial conditions. Here the volume of the deep water box is reduced to account for the formation of large continental ice shields. The depositional area on the continental shelf is diminished to simulate the effects of the marine regression. The sedimentation rates and depositional rates of terrigenous matter are changed because the locus of sedimentation was shifted from the shelves to the continental slope and rise under glacial conditions. Finally, the rate of dissolved phosphate input via dust deposition is enhanced to account for increased dust inputs. Corresponding parameter values (V_D, A, w, F_{PT}, F_{POCT}, F_{AEO}^{P}) are listed in Tables 5 and 6. The subsequent simulations G2 to G6 use the same parameter values as G1 but diminished f_{DS} values.

N_2-fixation in low-latitude surface waters. A further decrease in sealevel (simulations G5 and G6) has only a small effect on productivity because the nitrogen cycle is dominated by negative feedbacks reinforced by the redox dependence of denitrification. The final productivity is mainly defined by the maximum rate of N_2-fixation reached at low-N/P ratios in low-latitude surface waters. The model strongly suggests that the phosphate inventory was enlarged under glacial conditions due to a shift of POC deposition to deeper areas. Thus the model confirms an earlier hypothesis [*Broecker*, 1982] but offers a new explanation based on the modeling of redox-dependent benthic processes.

[36] High glacial dust inputs probably enhanced the delivery of dissolved iron to surface waters. Therefore the glacial productivity might have been higher in those areas of the global ocean where iron is the limiting nutrient [*Martin*, 1990] such as the polar Southern Ocean [*Watson et al.*, 2000]. A doubling of export efficiency at high southern latitudes with respect to the Holocene value is consistent with estimates of iron fluxes to the glacial ocean [*Mahowald et al.*, 1999]. The model was thus run with an increased kinetic constant for export production at high latitudes to simulate the effect of iron fertilization (Figure 6). This sensitivity test revealed the same nonlinear behavior as in the previous simulations. Thus a gradual increase in nutrient utilization slowly decreased the oxygen contents of deep waters until the threshold at ≈100 µM was overcome so that the deep water turned almost completely anoxic. Total

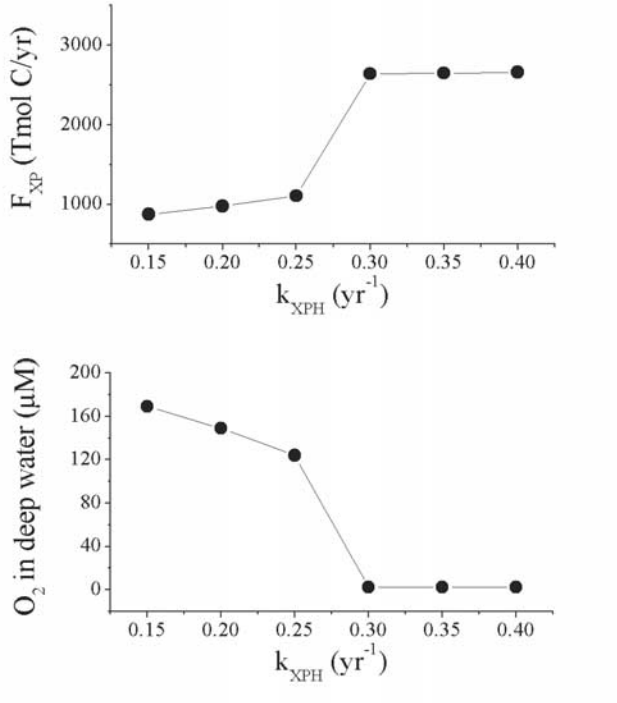

Figure 6. Changes in (top) export production and (bottom) deep water oxygen induced by the enhanced nutrient utilization at high latitudes (k_{XPH}) postulated for the glacial ocean. Steady state model runs were performed using the same parameter values as in simulation G1.

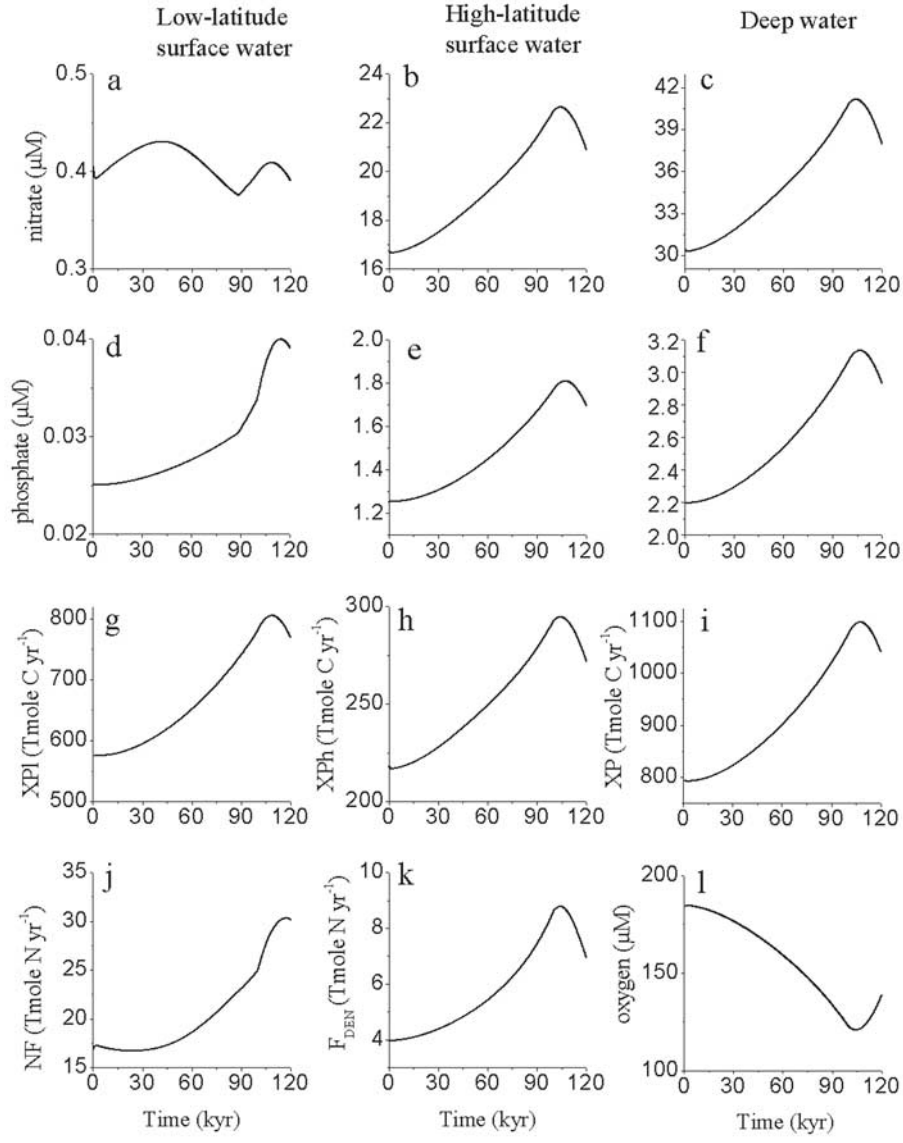

Figure 7. Pelagic model results of a nonsteady state model run simulating the effects of sea level change during a glacial cycle. Over the first 100 kyr of the simulation, parameters were changed linearly from Holocene to glacial values. During the glacial maximum at t = 100 kyr, the parameters attained the same values as in simulation G6 (Figure 5). Subsequently, they were readjusted linearly to Holocene values over the last 20 kyr of the simulation. Corresponding parameter values (f_{DS}, V_D, A, w, F_{PT}, F_{POCT}, F^P_{AEO}) are listed in Tables 5 and 6. (a) Dissolved nitrate in low-latitude surface water. (b) Dissolved nitrate in high-latitude surface water. (c) Dissolved nitrate in deep water. (d) Dissolved phosphate in low-latitude surface water. (e) Dissolved phosphate in high-latitude surface water. (f) Dissolved phosphate in deep water. (g) Export production at low latitudes. (h) Export production at high latitudes. (i) Total export production. (j) Nitrogen-fixation at low latitudes. (k) Denitrification in deep water. (l) Dissolved oxygen in deep water.

export production showed corresponding changes with a strong increase at low-oxygen levels caused by enhanced phosphate recycling at the seafloor.

[37] A nonsteady state simulation was run to explore the evolution of productivity and nutrient inventories through time as a result of changing sea level (Figure 7). The simulation started with interglacial (Holocene) parameter values. They were slowly and linearly changed from interglacial into glacial maximum values over the first 100 kyr of the model run to simulate the continuous drop in global sea level during the transition from interglacial to glacial maximum conditions. At t = 100 kyr, the parameters used

to drive the model attained the same values as in the steady state simulation G6 (Figure 5). Subsequently, the direction of change was inverted and the parameters were linearly readjusted to their Holocene values which were attained at the end of the simulation (at t = 120 kyr). Productivity and nutrient contents increased over the first 100 kyr because the fraction of export production deposited on the continental shelf was diminished continuously. In contrast to the corresponding steady state simulation, oxygen was only reduced to 120 μM and total export production was enhanced to only 1100 T mol yr^{-1} due to the restricted time available for the accumulation of high phosphate contents in deep water. The slow approach of steady state documented in Figure 7 clearly shows that the extremely high productivity and low-oxygen concentrations calculated for glacial boundary conditions were never fully attained during the late Quaternary because glacial periods were always terminated abruptly after a duration of about 100 kyr [*Petit et al.*, 1999]. Many box models as well as general circulation models with biogeochemical modules assume that the late Quaternary ocean has oscillated between a glacial and an interglacial steady state [e.g., *Archer et al.*, 2000a] even though estimates of Holocene fluxes suggest that the ocean has always been out of steady state during the Pleistocene and Holocene [*Codispoti*, 1995; *Milliman*, 1993; *Opdyke and Walker*, 1992]. The slow rate of change documented in Figure 7 supports the view that the late Quaternary ocean never reached a steady state because the equilibration time between ocean and sediments exceeds the available time span of 100 kyr. Steady state results (e.g., Figures 5–6) are thus of limited value.

[38] Moreover, the nonsteady state simulation (Figure 7) revealed that the high nutrient contents accumulated in the deep water box under glacial conditions (t = 0–100 kyr) were not fully consumed during the interglacial (t = 100–120 years). This result may be due to the poor representation of the events occurring during glacial terminations. In the model run, the glacial termination is marked by a reverse in the direction of sea level change only, whereas paleo climatic studies show that temperatures, pCO_2 values, sea-ice cover, and possibly also marine productivity and circulation started to change before the onset of sea level rise [*Broecker and Henderson*, 1998] with unknown consequences for the marine nutrient inventories.

[39] The benthic model results (Figure 8) reflect the changes in marine productivity and sedimentation rate over the model period. The POC/P_{reac} burial ratios peaked during the glacial maximum (at t = 100 kyr) and the highest maximum was observed in the continental slope and rise sediments. The author is not aware of a systematic sediment study investigating the changes in POC/P_{reac} burial ratio over glacial terminations. Such a study could be used to control the proposed model scenario.

[40] A large body of proxy data suggests that glacial deep-sea sediments and deep waters were indeed more reducing than their Holocene counterparts in extended areas of the global ocean. Evidences include low-Mn/Fe ratios in manganese nodules [*Bollhöfer et al.*, 1996; *Mangini et al.*, 1994], authigenic Mn maxima in sediments deposited during glacial terminations [*Berger et al.*, 1983; *Mangini et al.*, 2001; *Thomson et al.*, 1996; *Thomson et al.*, 1984; *Wallace et al.*, 1988; *Wilson et al.*, 1986], authigenic U enrichments in glacial sediments [*Francois et al.*, 1997; *Mangini et al.*, 2001; *Sarkar et al.*, 1993], enhanced concentrations and accumulation rates of POM [*Müller and Suess*, 1979; *Pedersen*, 1983; *Sarnthein et al.*, 1988], and changes in the abundance of sedimentary phosphorus phases [*Tamburini et al.*, 2002]. In contrast, water masses at shallow and intermediate depths were probably better ventilated during glacials [*Altabet et al.*, 1995; *Ganeshram et al.*, 1995; *Haug et al.*, 1998; *Sigman and Boyle*, 2000]. Considering that most glacial sediments were deposited at the deep seafloor and continental rise, the more reducing conditions in these deposits probably enhanced the benthic recycling of phosphate into the ocean [*Tamburini et al.*, 2002] allowing for a significant expansion of the dissolved phosphate inventory and a strong increase in marine productivity.

4.4. Exploring the Limits of Marine Productivity

[41] In the following section, the efficiency of nutrient utilization and the rates of N_2-fixation are varied to explore the limits of marine productivity. For this purpose, the formulation of the nitrogen cycle was further enhanced to consider the accumulation of ammonia in anoxic deep waters (Table 7).

[42] The efficiencies of nutrient utilization at high latitudes (k_{XPH}) and N_2-fixation at low latitudes (k_{FIX}) were varied systematically over several orders of magnitude (Figure 9). The productivity of the global ocean was changed by more than one order of magnitude upon this manipulation even though the input of nutrients from the continents into the oceans was maintained at a constant value corresponding to glacial boundary conditions. Eutrophic conditions with anoxic deep waters were obtained due to the positive feedback in the phosphorus cycle. Dissolved oxygen was almost completely exhausted when the export production rose above 3000 T mol POC yr^{-1}. Changes in the N_2-fixation rate had a strong effect on the productivity indicating that nitrate was the ultimate limiting nutrient over most of the investigated parameter space.

[43] Field studies and geological data clearly show that marginal seas and open oceans dominated by anoxic bottom waters are highly productive [*Arthur and Dean*, 1998; *Erbacher et al.*, 2001; *Haug et al.*, 1998; *Struck et al.*, 2001]. Usually, the anoxic conditions are ascribed to the high productivity whereas the source of nutrients is not identified even though additional phosphate supply from anoxic sediments could easily sustain and enhance eutrophic conditions in the overlying water. The role of phosphate recycling is clearly seen in the Black Sea and the Baltic Sea which are the most prominent examples of marginal seas with anoxic bottom waters. Here the POC/P_{reac} ratios are high in sediments deposited after the onset of anoxia so that the enhanced productivity may be supported and maintained by benthic phosphate release from surface sediments [*Arthur and Dean*, 1998; *Emeis et al.*, 2000]. Moreover, the analysis of Mediterranean sapropels showed that phases of enhanced productivity were accompanied and supported by anoxic conditions in bottom waters favoring

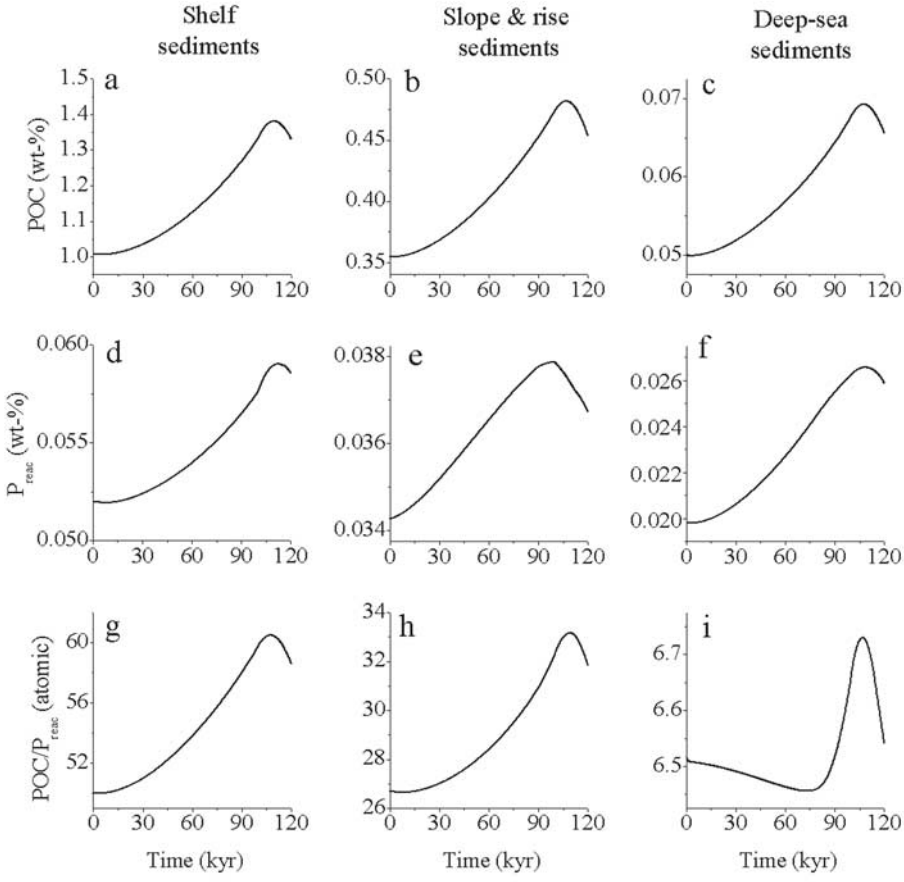

Figure 8. Benthic model results for the nonsteady state simulation (see Figure 7 for pelagic results and explanations). Concentrations of POC (a–c) and P_{reac} (d–f) at the lower boundary of the model columns (at 10 cm sediment depth) and the POC/P_{reac} burial ratios (g–i) in shelf, slope and rise, and deep-sea sediments are plotted as a function of time.

the release of benthic phosphate [C. P. Slomp et al., Controls on phosphorus regeneration and burial during formation of eastern Mediterranean sapropels, submitted to *Marine Geology*, 2002, hereinafter referred to as Slomp et al., submitted manuscript, 2002; *Slomp et al.*, 2002; *Struck et al.*, 2001].

5. Conclusions

[44] The ratio between POC and P_{reac} in marine sediments is strongly affected by the oxygen contents of the overlying bottom waters and by sedimentary redox conditions so that the POC/P_{reac} burial ratio increases by one order of magnitude under anoxic conditions. Enhanced productivity usually increases the burial ratio due to the enhanced benthic respiration and the shoaling penetration depths of oxygen and nitrate. The formation of authigenic P-bearing phases compensates for the enhanced phosphate release only at extremely high depositional rates of POC and P_{reac}. Thus the usual response of sediments to marine eutrophication is not enhanced burial and removal of P_{reac} as often assumed [*Ganeshram et al.*, 2002] but a strong reflux of dissolved phosphate into the overlying bottom water. This redox-dependent behavior induces a powerful positive feedback strongly affecting the productivity and redox-state of periodically anoxic marginal basins [*Emeis et al.*, 2000; Slomp et al., submitted manuscript, 2002; *Slomp et al.*, 2002; *Struck et al.*, 2001] and the productivity of the global ocean [*Ingall and Jahnke*, 1994; *Van Cappellen and Ingall*, 1994].

[45] The total export production of the global ocean and the size of the marine nutrient inventory can be increased by one order of magnitude by improving the efficiency of nutrient utilization at high latitudes and by enhancing N_2-fixation at low latitudes. This strong eutrophication may occur at constant rates of nutrient delivery from the continents. It is associated with a rapid spread of anoxia in deep waters and a massive burial of POC in marine sediments. Thus the marine biogeochemical system is not only subject to external perturbations but may strongly effect the global cycles of carbon, oxygen, and other elements due to internal feedbacks associated with the redox-dependent

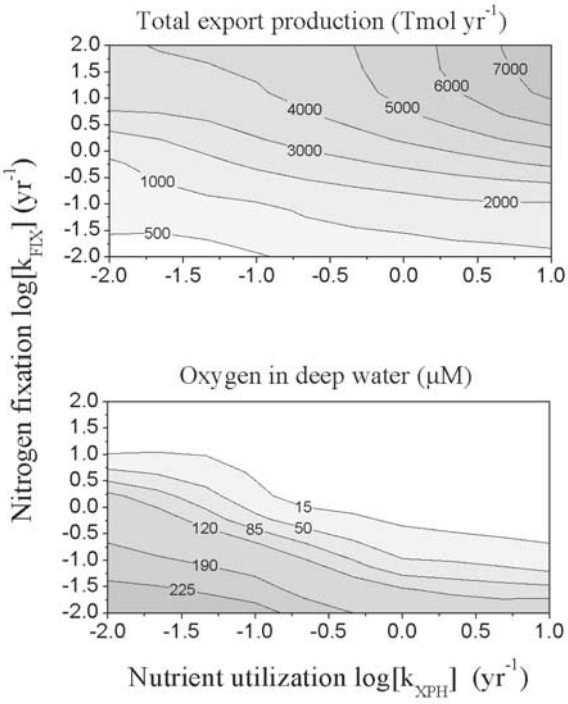

Figure 9. Impact of nutrient utilization and N_2-fixation on marine productivity and oxygen contents of bottom waters. The kinetic constant defining the efficiency of nutrient utilization at high latitudes (k_{XPH}) was varied from 0.02 to 20 yr^{-1} whereas the kinetic constant defining the efficiency of N_2-fixation (k_{FIX}) was varied from 0.01 to 100 yr^{-1}. Each of the contour plots is based on 20 individual model runs spanning a regular grid in the log(k_{XPH}) - log(k_{FIX})-plane. The simulations were run over model periods of several 100 kyr to approach steady state using the additional model equations defined in Table 7 and applying the glacial parameter values of simulation G1 (Figure 5).

phosphate turnover in marine sediments [*Betts and Holland*, 1991; *Holland*, 1984; *Van Cappellen and Ingall*, 1996; *Wallmann*, 2001].

[46] The phosphate inventory of the glacial ocean was enlarged due to a decrease in the oxygen contents of deep water masses caused by the exposure of continental shelf areas and by iron fertilization. Moreover, enhanced stratification at high latitudes might have decreased the ventilation of the deep ocean [*Sigman and Boyle*, 2000] and thereby the oxygen contents of deep waters. This would further increase the release of phosphate from sediments and the marine productivity. Thus glacial/interglacial changes in the global ocean's productivity are not inhibited by negative feedbacks and stoichiometric constraints as recently proposed [*Archer et al.*, 2000a] but may attain large amplitudes due to the positive feedback rooted in the redox-dependent benthic phosphorus cycle.

[47] In the modern ocean, the average ratio of dissolved nitrate to phosphate (15) is close to the N/P ratio observed in marine phytoplankton (16). This surprising observation has stimulated an incessant debate [*Lenton and Watson*, 2000; *Redfield*, 1958; *Tyrrell*, 1999]. The model results presented here suggest that N_2-fixation maintains the modern nutrient ratio under oxic conditions whereas the ratio decreases dramatically upon the spread of anoxia.

[48] A further long-standing debate is centered on the question whether marine productivity is ultimately limited by nitrate or phosphate [*Falkowski*, 1997; *Tyrrell*, 1999]. The model presented here shows that nitrate is limiting under eutrophic and reducing conditions while phosphate is the ultimate limiting nutrient in oligotrophic and oxic environments.

[49] Productivity and redox state of the ocean are linked via highly nonlinear relations. On one hand, an increase in the ocean's productivity results in enhanced nutrient removal via burial and denitrification. On the other hand, the nutrient inventory and the productivity may be further enhanced due to the benthic release of phosphate. A threshold value appears as a result of these negative and positive feedbacks. The ocean's productivity is maintained at moderate values accompanied by oxic conditions in deep waters as long as the oxygen content of the bottom waters is higher than 100 μM. Both eutrophic conditions and anoxia spread rapidly as soon as this threshold is overcome. The modern ocean is located close to this threshold and may thus reside on the brink of anoxia [*Lenton and Watson*, 2000].

[50] Recent data show that eutrophication of coastal waters has been increased in many areas leading to enhanced hypoxia in bottom waters, enhanced denitrification, and changes in the functional groups dominating the phytoplankton community [*Emeis et al.*, 2000; *Goolsby*, 2000; *Liu et al.*, 2000; *Naqvi et al.*, 2000; *Rabouille et al.*, 2001; *Ver et al.*, 1999b]. Moreover, the stratification of the upper water column in the equatorial Pacific has been enhanced over the last decades inducing a decrease in the ventilation of intermediate waters [*McPhaden and Zhang*, 2002]. Finally, it has been proposed to fertilize the Southern Ocean and other areas of the ocean with iron to increase the biological CO_2 uptake and to remove anthropogenic CO_2 from the atmosphere. All of these anthropogenic perturbations are amplified by the release of dissolved phosphate from anoxic sediments and may thus ultimately push significant areas of the global ocean toward anoxia. Thus the positive feedback rooted in the benthic phosphorus cycle has to be considered and should be more closely investigated in high-resolution models of the ocean to predict the consequences of iron-fertilization and other human impacts on the marine biogeochemical system.

[51] **Acknowledgments.** The author likes to thank E. Suess, J. Veizer, R.A. Berner, A. Eisenhauer, S. Kasten, R. Luff, and C. Hensen for stimulating discussions.

References

Altabet, M. A., R. Francois, D. W. Murray, and W. L. Prell, Climate-related variations in denitrification in the Arabian Sea from sediment $^{15}N/^{14}N$ ratios, *Nature*, *373*, 506–509, 1995.

Anderson, L. A., and J. L. Sarmiento, Redfield ratios of remineralization determined by nutrient data analysis, *Global Biogeochem. Cycles*, *8*(1), 65–80, 1994.

Anderson, L. D., M. L. Delaney, and K. L. Faul, Carbon to phosphorus ratios in sediments: Implications for nutrient cycling, *Global Biogeochem. Cycles*, *15*(1), 65–79, 2001.

Archer, D., A. Winguth, D. Lea, and N. Mahowald, What caused the glacial/interglacial atmospheric pCO_2 cycles?, *Rev. Geophys.*, *38*, 159–189, 2000a.

Archer, D. E., G. Eshel, A. Winguth, W. Broecker, R. Pierrehumbert, M. Tobis, and R. Jacob, Atmospheric pCO_2 sensitivity to the biological pump in the ocean, *Global Biogeochem. Cycles*, *14*(4), 1219–1230, 2000b.

Arthur, M. A., and W. E. Dean, Organic matter production and preservation and evolution of anoxia in the Holocene Black Sea, *Paleoceanography*, *13*(4), 395–411, 1998.

Berelson, W. M., D. E. Hammond, and K. S. Johnson, Benthic fluxes and the cycling of biogenic silica and carbon in two southern California borderland basins, *Geochim. Cosmochim. Acta*, *51*, 1345–1363, 1987.

Berger, W. H., R. C. Finkel, J. S. Killingley, and V. Marchig, Glacial-Holocene transition in deep-sea sediments: Manganese-spike in the east equatorial Pacific, *Nature*, *303*, 231–233, 1983.

Berner, E. K., and R. A. Berner, *Global Environment: Water, Air and Geochemical Cycles*, 376 pp., Prentice-Hall, Old Tappan, N.J., 1996.

Berner, R. A., and J.-J. Rao, Phosphorus in sediments of the Amazon River and estuary: Implications for the global flux of phosphorus to the sea, *Geochim. Cosmochim. Acta*, *58*, 2333–2339, 1994.

Betts, J. N., and H. D. Holland, The oxygen content of ocean bottom waters, the burial efficiency of organic carbon, and the regulation of atmospheric oxygen, *Palaeogeogr. Palaeoclimatol. Palaeoecol.*, *97*, 5–18, 1991.

Bollhöfer, A., A. Eisenhauer, N. Frank, D. Pech, and A. Mangini, Thorium and uranium isotopes in a manganese nodule from the Peru basin determined by alpha spectrometry and thermal ionization mass spectrometry (TIMS): Are manganese supply and growth related to climate?, *Geol. Rundsch.*, *85*, 577–585, 1996.

Boudreau, B. P., A method-of-lines code for carbon and nutrient diagenesis in aquatic sediments, *Comput. Geosci.*, *22*(5), 479–496, 1996.

Boudreau, B. P., *Diagenetic Models and Their Implementation*, 414 pp., Springer-Verlag, New York, 1997.

Broecker, W. S., Glacial to interglacial changes in ocean chemistry, *Prog. Oceanogr.*, *11*, 151–197, 1982.

Broecker, W. S., and G. M. Henderson, The sequence of events surrounding Termination II and their implications for the cause of glacial-interglacial CO_2 changes, *Paleoceanography*, *13*(4), 352–364, 1998.

Christensen, J. P., Benthic nutrient regeneration and denitrification on the Washington continental shelf, *Deep Sea Res., Part A*, *34*(5/6), 1027–1047, 1987.

Codispoti, L. A., Is the ocean losing nitrate?, *Nature*, *376*, 724, 1995.

Colman, A. S., and H. D. Holland, The global diagenetic flux of phosphorus from marine sediments to the oceans: Redox sensitivity and the control of atmospheric oxygen levels, in *Marine Authigenesis: From Global to Microbial*, Soc. of Sediment. Geol., Tulsa, Okla., 2000.

Cornell, S., A. Rendell, and T. Jickells, Atmospheric inputs of dissolved organic nitrogen to the oceans, *Nature*, *376*, 243–246, 1995.

Delaney, M. L., Phosphorus accumulation in marine sediments and the oceanic phosphorus cycle, *Global Biogeochem. Cycles*, *12*(4), 563–572, 1998.

Duce, R. A., et al., The atmospheric input of trace species to the world ocean, *Global Biogeochem. Cycles*, *5*(3), 193–259, 1991.

Emeis, K.-C., U. Struck, T. Leipe, F. Pollehne, H. Kunzendorf, and C. Christiansen, Changes in the C, N, P burial rates in some Baltic sea sediments over the last 150 years—Relevance to P regeneration rates and the phosphorus cycle, *Mar. Geol.*, *167*, 43–59, 2000.

Erbacher, J., B. T. Huber, R. D. Norris, and M. Markey, Increased thermohaline stratification as a possible cause for an ocean anoxic event in the Cretaceous period, *Nature*, *409*, 325–327, 2001.

Falkowski, P. G., Evolution of the nitrogen cycle and its influence on the biological sequestration of CO_2 in the ocean, *Nature*, *387*, 272–275, 1997.

Falkowski, P. G., R. T. Barber, and V. Smetacek, Biogeochemical controls and feedbacks on ocean primary production, *Science*, *281*, 200–206, 1998.

Filippelli, G. M., Controls on phosphorus concentration and accumulation in oceanic sediments, *Mar. Geol.*, *139*, 231–240, 1997.

Föllmi, K. B., H. Weissert, and A. Lini, Nonlinearities in phosphogenesis and phosphorus-carbon coupling and their implications for global change, in *Interactions of C, N, P and S Biogeochemical Cycles and Global Change*, edited by R. Wollast, F. T. Mackenzie, and L. Chou, pp. 447–474, Springer-Verlag, New York, 1993.

Frakes, L. A., J. E. Francis, and J. I. Syktus, *Climate Modes of the Phanerozoic*, 274 pp., Cambridge Univ. Press, New York, 1992.

Francois, R., M. A. Altabet, E.-F. Yu, D. M. Sigman, M. P. Bacon, M. Frank, G. Bohrmann, G. Bareille, and L.D. Labeyrie, Contribution of Southern Ocean surface-water stratification to low atmospheric CO_2 concentrations during the last glacial period, *Nature*, *389*, 929–935, 1997.

Ganeshram, R. S., T. F. Pedersen, S. E. Calvert, and J. W. Murray, Large changes in oceanic nutrient inventories from glacial to interglacial periods, *Nature*, *376*, 755–758, 1995.

Ganeshram, R. S., T. F. Pedersen, S. E. Calvert, and R. Francois, Reduced nitrogen fixation in the glacial ocean inferred from changes in marine nitrogen and phosphorus inventories, *Nature*, *415*, 156–159, 2002.

Goolsby, D. A., Mississippi Basin nitrogen flux believed to cause Gulf hypoxia, *Eos Trans. AGU*, *81*(29), 321, 2000.

Gruber, N., and J. L. Sarmiento, Global patterns of marine nitrogen fixation and denitrification, *Global Biogeochem. Cycles*, *11*(2), 235–266, 1997.

Haug, G. H., T. F. Pedersen, D. M. Sigman, S. E. Calvert, B. Nielsen, and L. C. Peterson, Glacial/interglacial variations in production and nitrogen fixation in the Cariaco Basin during the last 580 kyr, *Paleoceanography*, *13*(5), 427–432, 1998.

Hay, W. W., Pleistocene-Holocene fluxes are not the Earth's norm, in *Material Fluxes on the Surface of the Earth*, edited by W. W. Hay and T. Usselman, pp. 15–27, Natl. Acad. Press, Washington, D.C., 1994.

Hay, W. W., and J. R. Southam, Modulation of marine sedimentation by the continental shelves, in *The Fate of Fossil Fuel CO_2 in the Oceans*, edited by N. R. Andersen and A. Malahoff, pp. 569–604, Plenum, New York, 1977.

Hedges, J. I., and R. G. Keil, Sedimentary organic matter preservation: An assessment and speculative synthesis, *Mar. Chem.*, *49*, 81–115, 1995.

Hensen, C., H. Landenberger, M. Zabel, and H. D. Schulz, Quantification of diffusive benthic fluxes of nitrate, phosphate, and silicate in the southern Atlantic Ocean, *Global Biogeochem. Cycles*, *12*(1), 193–210, 1998.

Holland, H. D., *The Chemical Evolution of the Atmosphere and Oceans*, 582 pp., Princeton Univ. Press, Princeton, N.J., 1984.

Ingall, E. D., and R. A. Jahnke, Evidence for enhanced phosphorus regeneration from marine sediments overlain by oxygen depleted waters, *Geochim. Cosmochim. Acta*, *58*, 2571–2575, 1994.

Ingall, E. D., and R. A. Jahnke, Influence of water-column anoxia on the elemental fractionation of carbon and phosphorus during sediment diagenesis, *Mar. Geol.*, *139*, 219–229, 1997.

Ingall, E. D., and P. Van Cappellen, Relation between sedimentation rate and burial of organic phosphorus and organic carbon in marine sediments, *Geochim. Cosmochim. Acta*, *54*, 373–386, 1990.

Ingall, E. D., R. M. Bustin, and P. Van Cappellen, Influence of water column anoxia on the burial and preservation of carbon and phosphorus in marine shales, *Geochim. Cosmochim. Acta*, *57*, 303–316, 1993.

Jahnke, R. A., The global ocean flux of particulate organic carbon: Areal distribution and magnitude, *Global Biogeochem. Cycles*, *10*(1), 71–88, 1996.

Knox, F., and M. McElroy, Change in atmospheric CO_2: Influence of the marine biota at high latitude, *J. Geophys. Res.*, *89*, 4627–4637, 1984.

Lenton, T. M., and A. J. Watson, Redfield revisited: 1. Regulation of nitrate, phosphate, and oxygen in the ocean, *Global Biogeochem. Cycles*, *14*(1), 225–248, 2000.

Lisitzin, A. P., *Oceanic Sedimentation: Lithology and Geochemistry*, 400 pp., AGU, Washington, D.C., 1996.

Liu, K. K., L. Atkinson, C. T. A. Chen, S. Gao, J. Hall, R. W. Macdonald, L. T. McManus, and R. Quinones, Exploring continental margin carbon fluxes on a global scale, *Eos Trans. AGU*, *81*(52), 641, 2000.

Ludwig, W., P. Amiotte-Suchet, and J.-L. Probst, Enhanced chemical weathering of rocks during the Last Glacial Maximum: A sink for atmospheric CO_2?, *Chem. Geol.*, *159*, 147–161, 1999.

Luff, R., K. Wallmann, S. Grandel, and M. Schlüter, Numerical modelling of benthic processes in the deep Arabian Sea, *Deep Sea Res., Part II*, *47*(14), 3039–3072, 2000.

Mahowald, N., K. Kohfeld, M. Hansson, Y. Balkanski, S.P. Harrison, I.C. Prentice, M. Schulz, and H. Rodhe, Dust sources and deposition during the last glacial maximum and current climate: A comparison of model results with paleodata from ice cores and marine sediments, *J. Geophys. Res.*, *104*, 15,895–15,916, 1999.

Maier-Reimer, E., Geochemical cycles in an ocean general circulation model: Preindustrial tracer distribution, *Global Biogeochem. Cycles*, *7*(3), 645–677, 1993.

Mangini, A., H. J. Rutsch, M. Frank, A. Eisenhauer, and J. D. Eckhardt, Is there a relationship between atmospheric CO_2 and manganese in the ocean?, in *Carbon Cycling in the Glacial Ocean: Constraints in the Ocean's Role in Global Change*, *NATO ASI Ser.*, vol. 117, edited by R. Zahn, pp. 87–104, N. Atlantic Treaty Org., Brussels, 1994.

Mangini, A., M. Jung, and S. Laukenmann, What do we learn from peaks of uranium and of manganese in deep-sea sediments?, *Mar. Geol.*, *177*, 63–78, 2001.

Martin, J. H., Glacial-interglacial CO_2 change: The iron hypothesis, *Paleoceanography*, *5*(1), 1–13, 1990.

McElroy, M. B., Marine biological controls on atmospheric CO_2 and climate, *Nature*, *302*, 328–329, 1983.

McManus, J., W. M. Berelson, K. H. Coale, K. S. Johnson, and T. E. Kilgore, Phosphorus regeneration in continental margin sediments, *Geochim. Cosmochim. Acta*, *61*, 2891–2907, 1997.

McPhaden, M. J., and D. Zhang, Slowdown of the meridional overturning circulation in the upper Pacific Ocean, *Nature*, *415*, 603–608, 2002.

Menard, H. W., and S. M. Smith, Hypsometry of ocean basin provinces, *J. Geophys. Res.*, *71*, 4305–4325, 1966.

Meybeck, M., C, N, and P and S in rivers: From sources to global inputs, in *Interactions of C, N, P and S in Biogeochemical Cycles and Global Change*, edited by R. Wollast, F. T. Mackenzie, and L. Chou, pp. 163–193, Springer-Verlag, New York, 1993.

Middelburg, J. J., K. Soetaert, and P. M. J. Herman, Empirical relationships for use in global diagenetic models, *Deep Sea Res., Part I*, *44*(2), 327–344, 1996a.

Middelburg, J. J., K. Soetaert, P. M. J. Herman, and C. H. R. Heip, Denitrification in marine sediments: A model study, *Global Biogeochem. Cycles*, *10*(4), 661–673, 1996b.

Milliman, J. D., Production and accumulation of calcium carbonate in the ocean: Budget of a nonsteady state, *Global Biogeochem. Cycles*, *7*(4), 927–957, 1993.

Müller, P. J., and E. Suess, Productivity, sedimentation rate, and sedimentary organic matter in the oceans: I. Organic carbon preservation, *Deep Sea Res., Part A*, *26*, 1347–1362, 1979.

Naqvi, S. W. A., D. A. Jayakumar, P. V. Narvekar, H. Naik, V. V. S. S. Sarma, W. D'Souza, S. Joseph, and M. D. George, Increased marine production in N_2O due to intensifying anoxia on the Indian continental shelf, *Nature*, *408*, 346–349, 2000.

Opdyke, B. N., and J. C. G. Walker, Return of the coral reef hypothesis: Basin to shelf partitioning of $CaCO_3$ and its effect on atmospheric CO_2, *Geology*, *20*, 733–736, 1992.

Pedersen, T. F., Increased productivity in the eastern equatorial Pacific during the last glacial maximum, *Geology*, *11*, 16–19, 1983.

Peltier, W. R., Ice age paleotopography, *Science*, *265*, 195–201, 1994.

Petit, L. R., et al., Climate and atmospheric history of the past 420,000 years from the Vostok ice core, Antarctica, *Nature*, *399*, 429–436, 1999.

Rabouille, C., and J.-F. Gaillard, Towards the EDGE: Early diagenetic global explanation: A model depicting the early diagenesis of organic matter, O_2, NO_3, Mn, and PO_4, *Geochim. Cosmochim. Acta*, *55*, 2511–2525, 1991.

Rabouille, C., F. T. Mackenzie, and L. M. Ver, Influence of the human pertubation on carbon, nitrogen, and oxygen biogeochemical cycles in the global coastal ocean, *Geochim. Cosmochim. Acta*, *65*, 3615–3641, 2001.

Redfield, A. C., The biological control of chemical factors in the environment, *Am. Sci.*, *46*, 205–221, 1958.

Reimers, C. E., R. A. Jahnke, and D. C. McCorkle, Carbon fluxes and burial rates over the continental slope and rise off central California with implications for the global carbon cycle, *Global Biogeochem. Cycles*, *6*(2), 199–224, 1992.

Reimers, C., K. C. Ruttenberg, D. E. Canfield, M. B. Christianssen, and J. B. Martin, Porewater pH and authigenic phases formed in the uppermost sediments of the Santa Barbara Basin, *Geochim. Cosmochim. Acta*, *60*, 4037–4057, 1996.

Rohling, E. J., M. Fenton, F. J. Jorissen, P. Bertrand, G. Ganssen, and J. P. Caulet, Magnitudes of sea-level lowstands of the past 500,000 years, *Nature*, *394*, 162–165, 1998.

Rosenthal, Y., E. A. Boyle, L. Labeyrie, and D. Oppo, Glacial enrichments of authigenic Cd and U in Subantarctic sediments: A climatic control on the elements' oceanic budget?, *Paleoceanography*, *10*(3), 395–413, 1995.

Ruttenberg, K. C., Reassessment of the oceanic residence time of phosphorus, *Chem. Geol.*, *107*, 405–409, 1993a.

Ruttenberg, K. C., and R. A. Berner, Authigenic apatite formation and burial in sediments from non-upwelling, continental margin environments, *Geochim. Cosmochim. Acta*, *57*, 991–1007, 1993b.

Sanudo-Wilhelmy, S. A., A. B. Kustka, C. J. Gobler, D. A. Hutchins, M. Yang, L. Lwiza, J. Burns, D. G. Capone, J. A. Raven, and E. J. Carpenter, Phosphorus limitation of nitrogen fixation by Trichodesmium in the central Atlantic Ocean, *Nature*, *411*, 66–69, 2001.

Sarkar, A., S. K. Bhattacharya, and M. M. Sarin, Geochemical evidence for anoxic deep water in the Arabian Sea during the last glaciation, *Geochim. Cosmochim. Acta*, *57*, 1009–1016, 1993.

Sarmiento, J. L., and J. R. Toggweiler, A new model for the role of the oceans in determining atmospheric P_{CO2}, *Nature*, *308*, 621–624, 1984.

Sarnthein, M., K. Winn, J.-C. Duplessy, and M. R. Fontugne, Global variations of surface ocean productivity in low and mid latitudes: Influence on CO_2 reservoirs of the deep ocean and atmosphere during the last 21,000 years, *Paleoceanography*, *3*(3), 361–399, 1988.

Schlitzer, R., Applying the adjoint method for biogeochemical modeling: Export of particulate organic matter in the world ocean, in *Inverse Methods in Global Biogeochemical Cycles*, *Geophys. Monogr. Ser.*, vol. 114, edited by P. Kasibhatla et al., pp. 107–124, AGU, Washington, D.C., 2000.

Shackleton, N. J., J. Imbrie, and M. A. Hall, Oxygen and carbon isotope record of East Pacific core V19-30: Implications for the formation of deep water in the late Pleistocene North Atlantic, *Earth Planet. Sci. Lett.*, *65*, 233–244, 1983.

Siegenthaler, U., and T. Wenk, Rapid atmospheric CO_2 variations and ocean circulation, *Nature*, *308*, 624–626, 1984.

Sigman, D. M., and E. A. Boyle, Glacial/interglacial variations in atmospheric carbon dioxide, *Nature*, *407*, 859–869, 2000.

Slomp, C. P., J. Thompson, and G. De Lange, Enhanced regeneration of phosphorus during formation of the most recent eastern Mediterranean sapropel (S1), *Geochim. Cosmochim. Acta*, *66*, 1171–1184, 2002.

Smith, K. L., Jr., G. A. White, and M. B. Laver, Oxygen uptake and nutrient exchange of sediments measured in situ using a free vehicle grab respirometer, *Deep Sea Res., Part A*, *26*, 337–346, 1979.

Stein, R., J. Rüllkötter, and D. H. Welte, Accumulation of organic-carbon rich sediments in the late Jurassic and Cretaceous Atlantic Ocean—A synthesis, *Chem. Geol.*, *56*, 1–32, 1986.

Struck, U., K.-C. Emeis, M. Voß, M. D. Krom, and G. H. Rau, Biological productivity during sapropel S5 formation in the eastern Mediterranean Sea: Evidence from stable isotopes of nitrogen and carbon, *Geochim. Cosmochim. Acta*, *65*, 3249–3266, 2001.

Sundby, B., C. Gobeil, N. Silverberg, and A. Mucci, The phosphorus cycle in coastal marine sediments, *Limnol. Oceanogr.*, *37*(6), 1129–1145, 1992.

Tamburini, F., S. Huon, P. Steinmann, F. E. Grousset, T. Adatte, and K. B. Föllmi, Dysaerobic conditions during Heinrich events 4 and 5: Evidence from phosphorus distribution in a North Atlantic deep-sea core, *Geochim. Cosmochim. Acta*, *66*, 4069–4083, 2002.

Thomson, J., T. R. S. Wilson, F. Cullin, and D. J. Hydes, Non-steady state diagenetic record in eastern equatorial Atlantic sediments, *Earth Planet. Sci. Lett.*, *71*, 23–30, 1984.

Thomson, J., N. C. Higgs, and S. Colley, Diagenetic redistribution of redox-sensitive elements in northeast Atlantic glacial/interglacial transition sediments, *Earth Planet. Sci. Lett.*, *139*, 365–377, 1996.

Toggweiler, J. R., Variation of atmospheric CO_2 by ventilation of the ocean's deepest water, *Paleoceanography*, *14*(5), 571–588, 1999.

Tyrrell, T., The relative influences of nitrogen and phosphorus on oceanic primary production, *Nature*, *400*, 525–531, 1999.

Van Cappellen, P., and R. A. Berner, A mathematical model for the early diagenesis of phosphorus and fluorine in marine sediments: Apatite precipitation, *Am. J. Sci.*, *288*, 289–333, 1988.

Van Cappellen, P., and E. D. Ingall, Benthic phosphorus regeneration, net primary production, and ocean anoxia: A model of the coupled marine biogeochemical cycles of carbon and phosphorus, *Paleoceanography*, *9*(5), 677–692, 1994.

Van Cappellen, P., and E. D. Ingall, Redox stabilization of the atmosphere and oceans by phosphorus-limited marine productivity, *Science*, *271*, 493–496, 1996a.

Van Cappellen, P., and Y. Wang, Cycling of iron and manganese in surface sediments: A general theory for the coupled transport and reaction of carbon, oxygen, nitrogen, sulfur, iron, and manganese, *Am. J. Sci.*, *296*, 197–243, 1996b.

Ver, L. M. B., F. T. Mackenzie, and A. Lerman, Biogeochemical responses of the carbon cycle to natural and human perturbations: Past, present, and future, *Am. J. Sci.*, *299*, 762–801, 1999a.

Ver, L. M. B., F. T. Mackenzie, and A. Lerman, Carbon cycle in the coastal zone: Effects of global perturbations and change in the past three centuries, *Chem. Geol.*, *159*, 283–304, 1999b.

Wallace, H. E., J. Thomson, T. R. S. Wilson, P. P. E. Weaver, N. C. Higgs, and D. J. Hydes, Active diagenetic formation of metal-rich layers in N. E. Atlantic sediments, *Geochim. Cosmochim. Acta*, *52*, 1557–1569, 1988.

Wallmann, K., Controls on Cretaceous and Cenozoic evolution of seawater composition, atmospheric CO_2 and climate, *Geochim. Cosmochim. Acta*, *65*, 3005–3025, 2001.

Watson, A. J., D. C. E. Bakker, A. J. Ridgwell, P. W. Boyd, and C. S. Law, Effect of iron supply on Southern Ocean CO_2 uptake and implications for glacial atmospheric CO_2, *Nature*, *407*, 730–733, 2000.

Wheat, C. G., R. A. Feely, and M. J. Mottl, Phosphate removal by oceanic hydrothermal processes: An update of the phosphorus budget in the oceans, *Geochim. Cosmochim. Acta*, *60*, 3593–3608, 1996.

Wilson, T. R. S., J. Thomson, D. J. Hydes, S. Colley, F. Culkin, and J. Sorensen, Oxidation fronts in pelagic sediments: Diagenetic formation of metal-rich layers, *Science*, *232*, 972–975, 1986.

Yamanaka, Y., and E. Tajika, The role of the vertical fluxes of particulate organic matter and calcite in the oceanic carbon cycle: Studies using an ocean biogeochemical general circulation model, *Global Biogeochem. Cycles*, *10*(2), 361–382, 1996.

Zehr, J. P., J. B. Waterbury, P. J. Turner, J. P. Montoya, E. Omoregie, G. F. Steward, A. Hansen, and D. M. Karl, Unicellular cyanobacteria fix N_2 in the subtropical North Pacific Ocean, *Nature*, *412*, 635–638, 2001.

K. Wallmann, GEOMAR, Marine Environmental Geology, Wischhofstrasse 1–3, Kiel 24148, Germany. (kwallmann@geomar.de)